ROS are evolutionary conserved cell-to-cell signals

Yosef Fichman[1], Linda Rowland[2], Melvin J. Oliver[1], and Ron Mittler[1,3,*]

[1]Division of Plant Sciences and Technology, College of Agriculture Food and Natural Resources and Interdisciplinary Plant Group, Christopher S. Bond Life Sciences Center University of Missouri. 1201 Rollins St, Columbia, MO 65201, USA.

[2]Department of Surgery, University of Missouri School of Medicine, Christopher S. Bond Life Sciences Center, University of Missouri, 1201 Rollins St, Columbia, MO 65201, USA

Running title: Evolution of cell-to-cell ROS signaling

***Corresponding author:** Ron Mittler (mittlerr@missouri.edu)

Abstract

Cell-to-cell communication is fundamental to multicellular organisms, as well as to unicellular organisms living in a microbiome. It is thought to have evolved as a stress- or quorum-sensing mechanism in unicellular organisms. A unique cell-to-cell communication mechanism that uses reactive oxygen species (ROS) as a signal (termed the 'ROS wave') was recently identified in flowering plants. This process is essential for systemic signaling and plant acclimation to stress and can spread from a small group of cells to the entire plant within minutes. Whether this signaling process is found in other organisms is however unknown. Here we report that a ROS-mediated cell-to-cell signaling process, like the ROS wave, can be found in ferns, mosses, multicellular and unicellular algae, amoeba, and mammalian cells. We further show that this process can be triggered by extracellular H_2O_2 application and blocked by inhibition of NADPH oxidases, and that at least in unicellular algae growing as a lawn on an agar plate, it communicates important stress-response signals between cells. Taken together, our findings suggest that an active process of cell-to-cell ROS signaling, like the ROS wave, evolved before unicellular and multicellular organisms diverged. This mechanism could have communicated an environmental stress signal between cells and coordinated the acclimation response of cells living in a community. The finding of a signaling process, like the ROS wave, in mammalian cells further contributes to our understanding of different diseases and could impact the development of new drugs that target, for example cancer or heart disease.

Introduction

Cells communicate with each other in many ways. The exchange of signals between cells is thought to have evolved as part of a mechanism to control cell density (*e.g.,* quorum sensing; QS)[1,2], and/or as part of a response mechanism to changes in environmental conditions (*e.g.,* in cells living in a biofilm)[3,4]. Cell-to-cell communication can occur between cells of the same species or organism (*e.g.,* in a multicellular organism)[5,6], as well as between cells of different organisms (*e.g.,* during interactions of cells with different pathogens)[7,8]. Two of the most conserved cell-to-cell signaling pathways are paracrine, secretion of signals that are perceived by neighboring cells, and juxtacrine, communication between cells connected via tunneling nano tubes, gap junctions, or plasmodesmata[9–11]. Examples of these signaling pathways can be found in archaea, bacteria, unicellular eukaryotes, and multicellular organisms[12]. With the evolution of the vascular and nervous systems, paracrine signaling was extended to endocrine signaling, the release of signals into the bloodstream, and paracrine and juxtacrine signaling began to contribute to long distance signaling as part of electrical and chemical synapses[5,6]. In addition, autocrine signaling evolved as a mechanism for cells to regulate their own function[13]. Cell-to-cell signaling therefore plays an important role in coordinating the developmental and environmental responses of groups of neighboring cells, as well as cells that are remotely connected via blood vessels or neurons.

In vascular plants, that lack true nervous and circulatory systems, local cell-to-cell communication is primarily mediated by paracrine (via the apoplast and cell wall) and juxtacrine (via plasmodesmata; PD) signaling, while long distance signaling is mediated through the vascular system (phloem and xylem vessels, as well as their associated cells)[14,15]. Among the key signals exchanged by plant cells are different metabolites, small RNA and peptide molecules, hormones, calcium, volatile compounds, hydraulic pressure signals, membrane potential changes (electric signals), and reactive oxygen species (ROS)[14–18]. A unique cell-to-cell signaling mechanism discovered in plants is the 'ROS wave'[19–21]. The ROS wave is an auto-propagating cell-to-cell signaling pathway in which the initiating cell activates extracellular (apoplastic) ROS production via respiratory burst oxidase homologs [RBOHs; the plant homologs of NADPH oxidases (NOXs) of mammalian cells][19–21]. The ROS produced by this cell is then sensed by neighboring cells and triggers in them a similar enhanced ROS production process, resulting in the activation of a cascade or wave of cell-to-cell 'enhanced ROS production state' that spreads from the initiating cells/tissues over long distances, sometimes spanning the entire length of the plant[20,21]. The ROS wave was also recently shown to spread from one plant to another, when plants physically touch each other and conditions are sufficiently humid[22]. In addition to plasma membrane-localized RBOHs, the ROS wave requires the function of PD-localized proteins, different calcium channels, calcium signaling proteins, phytochrome B, and the plasma membrane (PM)-localized apoplastic ROS receptor H_2O_2-induced Ca^{2+} increases 1 (HPCA1) protein[21,23,24].

Numerous studies have shown that the ROS wave is linked to cell-to-cell calcium and electric signaling and that it is required for plant acclimation to stress (*e.g.,*[17,21,24–27]).

Because ROS are thought to have been present on Earth for billions of years and to have accompanied the evolution of unicellular and multicellular organisms[28–32], we hypothesized that ROS, and perhaps a ROS-driven cell-to-cell signaling mechanism, like the ROS wave, could have evolved early during the evolution of life on Earth. To test this hypothesis, we studied whether ROS, and in particular an active auto-propagating process of cell-to-cell signaling mediated by ROS (like the ROS wave in flowering plants), can be found in plant lineages that diverged early in the plant phylogeny, including gymnosperms, ferns, lycophytes, bryophytes, multi and unicellular algae, as well as across the animal lineages in amoeba and mammalian cells. Here we show that a ROS-mediated cell-to-cell signaling process can be found in many of these organisms and cells, suggesting that ROS are evolutionarily conserved cell-to-cell signals.

Results

ROS as rapid systemic signals in vascular plants

We previously identified and studied the ROS wave in several different angiosperm species including Arabidopsis, rice, tomato, maize, dandelion, and wheat[20,22,24,33]. However, whether ROS can function as a rapid systemic signal in gymnosperms, as well as other plant lineages is unknown. Here we show that a rapid systemic ROS signal can be triggered by a local treatment of high light (HL) stress in *Pinus sylvestris* (Pine, a Gymnosperm), *Azolla filiculoides* (Azolla, a fern), and *Selaginella moellendorffii* (Selaginella, a Lycopodiaceae; Figure 1). The average rate of the ROS signal measured in these organisms is 0.14 cm min^{-1} (Table S1), faster than the diffusion rate of H_2O_2 in water or biological systems (the diffusion coefficient of H_2O_2 in water or tissues is in the range of 1-2.5 10^{-5} cm^2 min^{-1})[34–36], supporting the active nature of this systemic ROS signal. The findings presented in Figure 1 suggest that rapid systemic ROS signaling is conserved across several different members of the vascular plant family and may have evolved before these lineages diverged from a common ancestor.

Rapid systemic ROS signaling in non-vascular plants

Although the ROS wave was shown to primarily propagate through the vascular bundles of Arabidopsis in response to a local HL stress treatment[37], in response to a local wounding or heat stress treatments it could

also propagate through non-vascular tissues (*i.e.,* mesophyll cells)[38]. We therefore extended our study to include Bryophytes (hornworts, liverworts, and mosses) that emerged from an early split in the diversification of land plants and lack lignified vascular tissues[39]. As shown in Figure 2, a localized treatment of HL caused the activation of a rapid systemic ROS signal in *Anthoceros agrestis* (a Hornwort), *Marchantia polymorpha* (a Liverwort), and *Physcomitrium patens* (Physcomitrella, a Moss), with an average velocity of 0.13 cm min^{-1} (Table S1). These findings suggest that rapid systemic ROS signals are conserved across all land plants and can spread in a systemic manner within or between plants, even in plants that lack a true vascular tissue.

Rapid systemic ROS signaling in multicellular algae and unicellular organisms

The findings that rapid systemic ROS signals are conserved among many land plants (Figures 1 and 2)[20,22,24,33] prompted us to test whether they can also be found in multicellular (*Chara vulgaris*) and unicellular (*Chlamydomonas reinhardtii*) algae. Multicellular and unicellular algae are known to use extracellular ROS as signals and contain NOX/RBOH enzymes[40,41]. As shown in Figures 3A and 3B, a localized treatment of HL stress caused the activation of a rapid systemic ROS response in *Chara vulgaris* grown in liquid medium (velocity of 0.14 cm min^{-1}; Table S1), as well as in *Chlamydomonas reinhardtii* grown as a lawn on an agar plate (velocity of 0.12 cm min^{-1}; Table S1). These findings suggest that ROS can be used as rapid systemic signals even by unicellular organisms and may have evolved as a cell-to-cell signaling mechanism before multicellularity emerged.

The findings that rapid systemic ROS signaling can be found in unicellular alga (Figure 3B) prompted us to test whether it can also be found in other unicellular organisms, such as the soil dwelling amoeba *Dictyostelium discoideum*, that contains NOX and uses extracellular ROS for signaling[41–43]. As shown in Figure 3C, a localized treatment of heat injury caused the activation of a rapid systemic ROS signal in the amoeba *Dictyostelium discoideum* grown on agar plates (velocity of 0.2 cm min^{-1}; Table S1).

Initiation and inhibition of the ROS wave in *Physcomitrella, Chlamydomonas*, and *Dictyostelium*

Two important characteristics of the ROS wave are that it can be triggered by a localized application of H_2O_2 and that once activated it can be blocked by the application of diphenyleneiodonium chloride (DPI; a broad-spectrum NOX/RBOH inhibitor) at a distant location away from its initiation site[19–21]. As shown in Figure 4, application of a 1 µl drop of 10 mM H_2O_2 to *Physcomitrella, Chlamydomonas*, or *Dictyostelium*, grown on agar plates, triggered a rapid systemic ROS signal. In contrast, application of mock buffer to cells,

129 or application of 1 µl drop of 10 mM H_2O_2 to agar plates that contain no cells, did not result in a ROS signal.
130 To further test for H_2O_2 diffusion on plates that had no cells grown on them (live cells are required for
131 H_2DCFDA to generate a signal)[44], we used 2',7'-dichlorodihydrofluorescein (DCF; OxyBurst; 50 µM)[19] to
132 image H_2O_2 in empty plates following the application of 1 ul of 1 mM, or 1 M H_2O_2. As shown in Figure
133 S1, we could not detect the 1 ul of 1 mM H_2O_2, a concentration that resulted in a detectable ROS signal in
134 plates with the different organisms (Figure 4) but were able to detect the 1 ul of 1 M H_2O_2. This finding
135 suggests that the living cells of the different organisms shown in Figure 4 amplified the 1 ul of 1 mM H_2O_2
136 to detectable levels.

137 To test the effect of the RBOH/NOX inhibitor DPI on the propagation of the rapid systemic ROS signal in
138 *Physcomitrella, Chlamydomonas*, or *Dictyostelium*, grown on agar plates, we applied water or DPI (50 µM)
139 in a 1 mm wide strip of agar to the middle of plates, waited 5 min and applied HL or heat injury at one end
140 of the plate (Figure 5A). As shown in Figure 5B, application of DPI (but not water) to the middle of the
141 plate blocked the progression of the cell-to-cell ROS signal. The findings presented in Figures 4 and 5
142 suggest that the rapid systemic ROS signal, observed as propagating from the initial site of HL or heat
143 injury on plates in the different organisms shown in Figures 2-4, is auto-propagating and resembles the
144 ROS wave discovered and studied in *Arabidopsis thaliana*[19–21,37,38].

145

146 **Functional analysis of the rapid cell-to-cell systemic ROS signal in *Chlamydomonas reinhardtii***

147 To test whether the systemic ROS signal observed in the unicellular alga *Chlamydomonas reinhardtii*
148 (Figures 3-5) can transfer a biologically relevant signal between different cells that are at two ends of the
149 signal path (*i.e.,* local and systemic, on two ends of the agar plate; Figure 6A), we applied HL stress to one
150 corner of a lawn of *Chlamydomonas* cells and sampled these cells, as well as cells that are on the other end
151 of the plate (Figure 6A). We then tested the expression of a HL-response small heat shock protein
152 (sHSP17.1) in cells located at the two ends of the signal path following the application of HL stress to one
153 end of the plate (stressed cells; local). As shown in Figure 6B, the expression of sHSP17.1 was elevated at
154 both ends of the signal path (local and systemic; Figure 6A) suggesting that the ROS wave signal connecting
155 these cells is conveying a stress response signal from the stressed cells (local) to the non-stressed cells
156 (systemic) that did not sense the stress.

157 To test whether inhibiting the ROS wave in *Chlamydomonas* growing on an agar plate (Figure 5) would
158 inhibit the transfer of the stress-response signal from one side of the plate to the other (Figure 6B), we
159 applied DPI (50 µM) or water at the middle point between the stressed cells and the cells that did not sense
160 the stress (similar to Figure 5; Figure 6A). As shown in Figure 6C, DPI, but not water, inhibited the

161 expression of sHSP17.1 in the non-stressed (systemic) cells following the application of HL stress to the
162 stressed cells (local) that are on the other end of the plate. In contrast, DPI or water did not inhibit the
163 expression of sHSP17.1 at the stressed cells (local). These findings suggest that the cell-to-cell ROS signal
164 connecting the two ends of the *Chlamydomonas* lawn growing on the agar plate transfers biologically
165 relevant signals between cells.

166

167 **Cell-to-cell ROS signaling in mammalian cells**

168 The findings that the ROS wave could be found in the amoeba *Dictyostelium discoideum* (Figure 3C),
169 demonstrated that organisms that are outside the plant and algal lineages could use ROS as a cell-to-cell
170 signaling mechanism. *Dictyostelium discoideum* was previously found to contain an ancestral form of
171 NOX[28,41,43], suggesting that other organisms that contain NOX enzymes (for example mammalian cells)
172 could be using ROS for rapid cell-to-cell signaling. To test this possibility, we studied cell-to-cell ROS
173 signaling in monolayers of human (*Homo sapiens*) epithelial breast cancer (MDA-MB-231), and rat (*Rattus*
174 *norvegicus*) cardiomyocytes (H9c2), cells grown in culture. As shown in Figure 7A, wounding of a
175 monolayer of MDA-MB-231 or H9c2 cells with a heated rod resulted in a ROS signal that spread from the
176 injury site at a velocity of 0.28 or 0.2 cm min^{-1} (Table S1), respectively. In the case of H9c2 cells, the ROS
177 signal appeared to travel away from the wound site and to do so in a directional manner, suggesting that the
178 ROS signal observed is not simply ROS that are diffusing away from the initial wound site (Figure 7A;
179 Movie S1). To determine that the spreading ROS signal was not a result of cell migration and/or monolayer
180 detachment, we conducted microscopic analysis of H9c2 cells at the end the ROS imaging experiments.
181 This analysis revealed that the wound site had an average diameter of 300-600 μm and that cells did not
182 detach or migrate away from it (Figure S2). Moreover, migration of cells away from the wound site would
183 have been much slower (1–10 μm min^{-1})[45] than the rate of the signal observed (0.2 cm min^{-1}; Table S1). In
184 addition, to test that H_2O_2 can be detected in all H9c2 cells on the plates (not only the cells observed
185 generating ROS after wounding; Figure 7A), we treated the entire plate with a final concentration of 1 mM
186 H_2O_2 at the end of the experiment (Figure S3). This analysis revealed that all cells on the plate were able to
187 uptake the H_2DCFDA dye, and that H_2O_2 that was provided to the media and entered cells generated a
188 signal [for H_2DCFDA to generate a fluorescent signal at the rapid rate the signal is developing (Figure 7A),
189 it has to enter live cells][44]. To test whether the ROS signal observed in MDA-MB-231 or H9c2 is associated
190 with NOX function, we applied DPI (50 μM) or buffer (mock) to these cells prior to the heat injury. As
191 shown in Figure 7B, DPI, but not buffer, caused the complete suppression of the ROS signal.

192

Discussion

The steady-state level of ROS in cells can vary in response to different environmental conditions, the activation of developmental programs that cause active production of ROS, and/or a decline in the activity of ROS scavenging mechanisms[46–48]. ROS can also diffuse into or out of cells through aquaporins, further impacting intracellular ROS levels[47,48]. Because ROS affect the redox state of cells and can alter gene expression through oxidative post-translational modifications (oxi-PTMs) of different proteins[47], they function as key signal transduction molecules involved in the sensing of stress and/or the activation of different developmental programs[48].

Because ROS can be transported in or out of cells through aquaporins and/or other channels/pores, secretion of ROS by one cell can alter the redox state of a neighboring cell, thereby altering gene expression within it. This type of paracrine signaling is thought to play an important role in cell-to-cell signaling occurring in different communities of microorganisms, during algal blooms, during interactions between neurons, or during the recruitment of leukocytes to wound sites[49–53]. A central feature of this paracrine signaling mechanisms is, however, that it is dependent on a gradient of ROS forming from the secreting cell to the accepting cell(s). In addition, ROS can be scavenged in route from one cell to the other, limiting the range of this signaling pathway. Having the ability to amplify and maintain cell-to-cell ROS signals, like the auto-propagating ROS wave process in plants[19–21,37,38], would improve the communication between cells in a biofilm/community/tissue and allow them to respond faster and in unison (Figure 8). Here we demonstrate that *Physcomitrella, Chlamydomonas*, and *Dictyostelium*, growing on agar plates, and mammalian cells growing in culture, indeed have the capacity to amplify and maintain cell-to-cell ROS signals (Figures 3-7). This finding suggests that the ROS wave signaling process, that was originally discovered in flowering plants[19–21,37,38], could have originated early in evolution and is conserved between plants, microorganisms, and animal cells. In support of these data are the findings that the systemic ROS signal could be initiated by H_2O_2 (Figure 4), and that application of DPI at a location that is away from the initiation site could block it (Figure 5). Moreover, in H9c2 cells, the peak of the ROS signal propagated in a directional manner at a rate of 0.2 cm min^{-1} departing from its original initiation site and continuing to move away from it in a manner that clearly suggests it is not mediated by simple diffusion (Figures 7 and S3; Movie S1). Although the directionality of the ROS signal (Figures 7 and S3; Movie S1) could be related to cell polarity, it is unknown at present what is the mechanism that govern it.

An interesting analogy to the cell-to-cell ROS wave signaling process of plants is the synchronized process of mitochondrial ROS flushes that occurs in mitochondria that are arranged in a lattice formation in muscle tissue (*e.g.,* [54,55]). In this process the release of ROS through pores from one mitochondrion results in the release of ROS from a neighboring mitochondrion spreading from mitochondria-to-mitochondria in a ROS-

226 induced-ROS-release fashion[54,55]. In the context of our findings, that a similar process of cell-to-cell ROS
227 signaling occurs in many different unicellular and multicellular organisms (Figures 1-7), it is possible that
228 even ancient prokaryotic organisms that were the progenitors of mitochondria used this type of cell-to-cell
229 signaling to orchestrate responses within a biofilm or a colony. It is also possible that mitochondria are
230 actively involved in the cell-to-cell ROS signal found in H9c2 cells (Figure 7), and that NOXs such as
231 NOX4 that is associated with mitochondria in mammalian cells[56] are mediating this process. Further studies
232 are needed to address the potential role of mitochondria in cell-to-cell ROS signaling.

233 In addition to paracrine signaling, cells can use juxtacrine signaling to exchange ROS with each other[57]. To
234 use this route, however, the levels of ROS transported cannot be too high, as the transmitting or receiving
235 cells could be damaged. Cells living within a biofilm, colony, and/or within different plant and animal
236 tissues, are thought to use juxtacrine signalling to mediate cell-to-cell ROS and redox signaling[10,11].
237 Moreover, it was suggested that ROS can enhance the size of tunneling nanotubes or PDs and facilitate
238 juxtacrine signalling[23,57]. Because we did not distinguish between paracrine and juxtacrine signalling, we
239 cannot rule out the possibility that the cells we imaged used one or the other, or both, for the process of
240 cell-to-cell ROS signaling. In this respect it should be mentioned that our studies of the ROS wave in plants
241 have shown that for cell-to-cell paracrine ROS signaling to occur, juxtacrine signalling must also occur, as
242 key proteins localized to the PD must be present[23]. Paracrine and juxtacrine signalling might therefore be
243 linked in other organisms and this aspect of cell-to-cell ROS signaling should be addressed in future studies.

244 Cancer cells use ROS to regulate their own proliferation and to communicate with cancer-associated
245 macrophages and other host cells (*e.g.,* [58]). In addition, ROS plays a key role in cancer metastasis (*e.g.,* [59]).
246 Our findings that cancer cells can generate and transmit long distance ROS signals (Figure 7), could suggest
247 that a similar process may occur within the tumor microenvironment. This finding should be further studied
248 as it may affect the development of new cancer fighting drugs. In the heart, ROS were implicated in
249 ischemia reperfusion (IR) injury, both in the acute setting of myocardial infarction (MI), as well as in the
250 chronic remodeling process following a MI (*e.g.,* [60–62]). Our findings that cardiomyocytes can use ROS for
251 cell-to-cell communication (Figure 7; Movie S1), could suggest that enhanced ROS production during IR
252 could trigger different ROS signals that would augment or suppress the tissue damage caused during IR
253 injury. This finding should also be further studied as it could lead to the development of new therapies that
254 will limit tissue damage during IR.

255 Taken together, our findings suggest that cell-to-cell ROS signaling evolved before unicellular and
256 multicellular organisms diverged (Figures 1-7)[19–24]. Because ROS are thought to have been present on Earth
257 for billions of years and could be used to sense the cell's environment through changes in the redox status
258 of the cell[28,32,47,48], it is possible that a cell-to-cell process that uses ROS as a signal evolved early in

evolution. This mechanism could have communicated an environmental stress signal that altered the redox state of one cell (the initiating cell) through ROS secreted or transported by this cell to an acceptor cell (Figure 8). The changes in redox state caused by the perceived ROS signal in the acceptor cell would therefore have 'mirrored' the redox state of the initiating cell and information in the form of a 'redox change' transmitted from one cell to the other (Figure 8). The changes in redox state occurring in each of the two cells could cause ROS accumulation and activate gene expression through oxi-PTMs linking the gene expression and ROS responses of both cells (Figure 8). Since the redox state of other neighboring cells will also be altered in a similar manner during this process (like the redox changes that occur in cells along the path of the ROS wave in plants)[63], and these cells will also start accumulating and secreting ROS, the entire colony, biofilm, or tissue would respond in unison to the stress perceived by the initiating cell (Figure 8), improving its chances of acclimation to the sensed stress, as well as overall survival. Such a mechanism could have coordinated the redox and ROS accumulation responses of a network of cells and give this cell population a better chance of survival in the early environment that was present on Earth; and may have been conserved in one form or another in different organisms to date (Figures 1-7)[19–24]. ROS such and H_2O_2 could have therefore served as one of the first 'stress hormones' on Earth; and to induce a response, the level of this stress hormone (*i.e.,* H_2O_2) had to be increased (Figures 1-8). Our findings that an inhibitor of NADPH oxidases (DPI) can inhibit this process in different organisms (Figures 5-7), support the active nature of this process[19–21]. In addition, at least in *Chlamydomonas* we show that the cell-to-cell ROS signal is required for the expression of sHSP17.1 in cells that were not directly subjected to the stress (Figure 6), demonstrating that the systemic cell-to-cell ROS signal conveys important biological information between cells. In future studies it would be interesting to dissect this signaling process in different organisms and to determine whether it is dependent on paracrine, juxtacrine, or a combination of both signaling pathways (as in plants[20,21,23]). In addition, the nature of the ROS producing, transporting, and perceiving mechanisms need to be determined in different organisms. In plants these were found to be RBOHD/RBOHF, aquaporin PIP2;1, and HPCA1, respectively[19–21,23,37].

Methods

Organisms and stress treatments

The following organisms were studied in this research: *Pinus sylvestris* (TreeHelp, Buffalo, NY, USA); *Azolla filiculoides* (Carolina Biological Supply Company, Burlington, NC, USA), *Selaginella moellendorffii* (Putnam Hill nursery, Forest Hill, MD, USA), *Marchantia polymorpha* (Carolina Biological

291 Supply Company, Burlington, NC, USA), *Anthoceros agrestis* (a kind gift from Prof. Fay-Wei Li, Cornell
292 University), *Physcomitrium patens* (a kind gift from Prof. Elisabeth Haswell, Washington University at St.
293 Louis and International Moss Stock Center, Prof. Ralf Reski, University of Freiburg, Freiburg, Germany),
294 *Chara vulgaris* (Carolina Biological Supply Company, Burlington, NC, USA), *Chlamydomonas reinhardtii*
295 (UTEX Culture Collection of Algae, Austin, TX, USA), *Dictyostelium discoideum* (a kind gift from Prof.
296 Thierry Soldati, University of Geneva and Carolina Biological Supply Company, Burlington, NC, USA),
297 H9c2 and MDA-MB-231 (ATCC, Manassas, VA, USA). Organisms were grown according to stock
298 resource instructions. Photosynthetic organisms were grown under 8 hrs/ 16 hrs light/dark regime. *P.*
299 *sylvestris, S. moellendorffii and M. polymorpha* were grown in peat pellets (Jiffy-7, Jiffy International,
300 Kristiansand, Norway)[20,21]. *A. filiculoides* was grown on 0.25 MS liquid media[64]; *A. agrestis* was grown on
301 a solid modified Hatcher medium[65]; *P. patens* was grown on BCD solid media[66]; *Chara vulgaris* was grown
302 in a Broyer and Barr liquid media[67]; *C. reinhardtii* cultures were grown on P49 solid media (UTEX Culture
303 Collection of Algae, Austin, TX, USA); *D. discoideum* cultures were grown on SM agar plates in room
304 temperature[68]. Mammalian cells were grown in 37°C 5% CO_2 RPMI medium 1640 supplemented with 10%
305 FCS, L- glutamine, and antibiotics (ThermoFisher, Waltham, MA)[69]. A day before the experiment the
306 media was replaced with FluoroBrite DMEM (ThermoFisher, Waltham, MA) to reduce background
307 fluorescence[70]. For organisms treated with local HL stress, following fumigation with H_2DCFDA solution,
308 illumination of 1700 µmol photons m^{-2} s^{-1} was applied to a local leaf/area for 2 min using fiber optics
309 (Schott, Southbridge, MA, USA), as described previously[20,23,27,37]. Heat injury, following treatment of
310 H_2DCFDA was applied for *D. discoideum* and mammalian cells using an open-flame-heated metal rod that
311 touched the local injury area for 1 second[22]. Hydrogen peroxide was applied as a 1 µl drop of 10 mM diluted
312 in the buffer of the medium in which the organism was cultured. DPI (50 µM) or water were applied as a
313 strip of 0.05% agarose (applied with a pipette tip along the center of the plate; Figure 5A) for *P. patens*, *C.*
314 *reinhardtii* and *D. discoideum*, or in the media for mammalian cells 5-10 min prior to the stress
315 application[20].

316 **ROS imaging**

317 All organisms, outside of the mammalian cells, were fumigated with 50 µM H_2DCFDA (Millipore-Sigma,
318 St. Louis, MO, USA) in 0.05 M Phosphate buffer pH 7.4 with 0.01% Silwet L-77. Fumigation was carried
319 out for 30 min using nebulizers (Punasi Direct, Hong Kong, China)[20–24,37,38]. For mammalian cells 10 µM
320 H_2DCFDA (final concentration) was applied to the medium and incubated for 30 min. Following
321 H_2DCFDA fumigation/application, local stress was applied, and organisms were imaged for live ROS
322 accumulation using the IVIS Lumina S5 platform[20–24,37,38]. Acquired images were then analyzed using the
323 math function in Living Image software (PerkinElmer, Waltham, MA, USA) [20–24,37,38]. Empty agar plates

were also fumigated with 2',7'-dichlorodihydrofluorescein (DCF; OxyBurst; 50 μM)[19], treated with H_2O_2 and imaged as described above.

Protein blot analysis

Local and systemic cells of *C. reinhardtii* from treated or untreated plates, with or without DPI, 2 min or 30 min after a 2 min HL treatment were collected and denaturized by boiling in 4 x Laemmli buffer. The samples were spun down and the supernatant was loaded on SDS-PAGE and blotted to PVDF membrane. Polyclonal anti-sHSP17.1 antibodies from rabbit were used to identify the proteins on the membrane as described previously[24,25].

Statistical analysis

All experiments were repeated at least three times with at least 3 biological repeats. Box plots graphs are presented with mean as X ± SE; median is line in the box and box borders are 25th and 75th percentiles; whiskers are the 1.5 interquartile range. Paired Student t-test was conducted using Microsoft Excel (*$P < 0.05$; **$P < 0.01$; ***$P < 0.001$).

Acknowledgements

We thank Professor Brent Mishler for discussions regarding which plants to target for our evolutionary analysis. We also thank Professor Thierry Soldati for gift of *Dictyostelium discoideum*, Professor Elisabeth Haswell and Professor Ralf Reski for gift of *Physcomitrium patens*, and Professor Fay-Wei Li for gift of *Anthoceros agrestis*.

Funding

This work was supported by funding from the National Science Foundation grants IOS-2110017, IOS-1932639, and the Interdisciplinary Plant Group, University of Missouri.

349 **References**

350 1. Miller, M.B., and Bassler, B.L. (2001). Quorum sensing in bacteria. Annu. Rev. Microbiol. *55*, 165–
351 199.

352 2. Fan, Q., Wang, H., Mao, C., Li, J., Zhang, X., Grenier, D., Yi, L., and Wang, Y. (2022). Structure and
353 signal regulation mechanism of interspecies and interkingdom quorum sensing system receptors. J.
354 Agric. Food Chem. *70*, 429–445.

355 3. Gambino, M., and Cappitelli, F. (2016). Mini-review: Biofilm responses to oxidative stress. Biofouling
356 *32*, 167–178.

357 4. Mahto, K.U., Kumari, S., and Das, S. (2022). Unraveling the complex regulatory networks in biofilm
358 formation in bacteria and relevance of biofilms in environmental remediation. Crit. Rev. Biochem.
359 Mol. Biol. *57*, 305–332.

360 5. Holland, N.D. (2003). Early central nervous system evolution: an era of skin brains? Nat. Rev.
361 Neurosci. *4*, 617–627.

362 6. Ovsepian, S.V., O'Leary, V.B., and Vesselkin, N.P. (2020). Evolutionary origins of chemical synapses.
363 Vitam. Horm. *114*, 1–21.

364 7. Chávez, A.S.O., O'Neal, A.J., Santambrogio, L., Kotsyfakis, M., and Pedra, J.H.F. (2019). Message in
365 a vesicle - trans-kingdom intercommunication at the vector-host interface. J. Cell Sci. *132*, jcs224212.

366 8. Zhou, Q., Ma, K., Hu, H., Xing, X., Huang, X., and Gao, H. (2022). Extracellular vesicles: Their
367 functions in plant–pathogen interactions. Mol. Plant Pathol. *23*, 760–771.

368 9. Marchionni, M.A. (2014). Neuregulin signaling in pieces-evolution of the gene family. Curr. Pharm.
369 Des. *20*, 4856–4873.

370 10. Matkó, J., and Tóth, E.A. (2021). Membrane nanotubes are ancient machinery for cell-to-cell
371 communication and transport. Their interference with the immune system. Biol. Futura *72*, 25–36.

372 11. Ariazi, J., Benowitz, A., De Biasi, V., Den Boer, M.L., Cherqui, S., Cui, H., Douillet, N., Eugenin,
373 E.A., Favre, D., Goodman, S., et al. (2017). Tunneling Nanotubes and Gap junctions-their role in long-
374 range intercellular communication during development, health, and disease conditions. Front. Mol.
375 Neurosci. *10*, 333.

376 12. Combarnous, Y., and Nguyen, T.M.D. (2020). Cell communications among microorganisms, plants,
377 and animals: Origin, evolution, and interplays. Int. J. Mol. Sci. *21*, E8052.

378 13. Ghanam, J., Chetty, V.K., Barthel, L., Reinhardt, D., Hoyer, P.-F., and Thakur, B.K. (2022). DNA in
379 extracellular vesicles: from evolution to its current application in health and disease. Cell Biosci. *12*,
380 37.

381 14. Anfang, M., and Shani, E. (2021). Transport mechanisms of plant hormones. Curr. Opin. Plant Biol.
382 *63*, 102055.

383 15. Furumizu, C., Krabberød, A.K., Hammerstad, M., Alling, R.M., Wildhagen, M., Sawa, S., and Aalen,
384 R.B. (2021). The sequenced genomes of nonflowering land plants reveal the innovative evolutionary
385 history of peptide signaling. Plant Cell *33*, 2915–2934.

386 16. Farmer, E.E., Gao, Y.-Q., Lenzoni, G., Wolfender, J.-L., and Wu, Q. (2020). Wound and
387 mechanostimulated electrical signals control hormone responses. New Phytol. *227*, 1037–1050.

388 17. Fichman, Y., and Mittler, R. (2021). Integration of electric, calcium, reactive oxygen species and
389 hydraulic signals during rapid systemic signaling in plants. Plant J. *107*, 7–20.

390 18. Shao, Q., Gao, Q., Lhamo, D., Zhang, H., and Luan, S. (2020). Two glutamate- and pH-regulated Ca2+
391 channels are required for systemic wound signaling in Arabidopsis. Sci. Signal. *13*, aba1453.

392 19. Miller, G., Schlauch, K., Tam, R., Cortes, D., Torres, M.A., Shulaev, V., Dangl, J.L., and Mittler, R.
393 (2009). The plant NADPH oxidase RBOHD mediates rapid systemic signaling in response to diverse
394 stimuli. Sci. Signal. *2*, ra45–ra45.

395 20. Fichman, Y., Miller, G., and Mittler, R. (2019). Whole-plant live imaging of reactive oxygen species.
396 Mol. Plant *12*, 1203–1210.

397 21. Fichman, Y., Zandalinas, S.I., Peck, S.C., Luan, S., and Mittler, R. (2022). HPCA1 is required for
398 systemic ROS and calcium cell-to-cell signaling and plant acclimation to stress. Plant Cell,
399 10.1093/plcell/koac241.

400 22. Szechynska-Hebda, M., Lewandowska, M., Witoń, D., Fichman, Y., Mittler, R., and Karpinski, S.
401 (2022). Aboveground plant-to-plant electrical signaling mediates network acquired acclimation. Plant
402 Cell *34*, 3047–3065.

403 23. Fichman, Y., Myers, R.J., Grant, D.G., and Mittler, R. (2021). Plasmodesmata-localized proteins and
404 ROS orchestrate light-induced rapid systemic signaling in Arabidopsis. Sci. Signal. *14*, eabf0322.

405 24. Fichman, Y., Xiong, H., Sengupta, S., Azad, R.K., Hibberd, J.M., Liscum, E., and Mittler, R. (2021).
406 Phytochrome B regulates reactive oxygen signaling during abiotic and biotic stress in plants. BioRxiv,
407 2021.11.29.470478.

408 25. Suzuki, N., Miller, G., Salazar, C., Mondal, H.A., Shulaev, E., Cortes, D.F., Shuman, J.L., Luo, X.,
409 Shah, J., Schlauch, K., et al. (2013). Temporal-spatial interaction between reactive oxygen species and
410 abscisic acid regulates rapid systemic acclimation in plants. Plant Cell *25*, 3553–3569.

411 26. Zandalinas, S.I., Sengupta, S., Burks, D., Azad, R.K., and Mittler, R. (2019). Identification and
412 characterization of a core set of ROS wave-associated transcripts involved in the systemic acquired
413 acclimation response of Arabidopsis to excess light. Plant J. *98*, 126–141.

414 27. Zandalinas, S.I., Fichman, Y., Devireddy, A.R., Sengupta, S., Azad, R.K., and Mittler, R. (2020).
415 Systemic signaling during abiotic stress combination in plants. Proc. Natl. Acad. Sci. U.S.A. *117*,
416 13810–13820.

417 28. Inupakutika, M.A., Sengupta, S., Devireddy, A.R., Azad, R.K., and Mittler, R. (2016). The evolution
418 of reactive oxygen species metabolism. J. Exp. Bot. *67*, 5933–5943.

419 29. Taverne, Y.J., Merkus, D., Bogers, A.J., Halliwell, B., Duncker, D.J., and Lyons, T.W. (2018).
420 Reactive oxygen species: Radical factors in the evolution of animal life. BioEssays *40*, 1700158.

421 30. Hörandl, E., and Speijer, D. (2018). How oxygen gave rise to eukaryotic sex. Proc. Royal Soc. B *285*,
422 20172706.

423 31. Gutteridge, J.M.C., and Halliwell, B. (2018). Mini-Review: Oxidative stress, redox stress or redox
424 success? Biochem. Biophys. Res. Commun. *502*, 183–186.

425 32. Jabłońska, J., and Tawfik, D.S. (2021). The evolution of oxygen-utilizing enzymes suggests early
426 biosphere oxygenation. Nat. Ecol. Evol. *5*, 442–448.

427 33. Fichman, Y., and Mittler, R. (2020). Noninvasive live ROS imaging of whole plants grown in soil.
428 Trends Plant Sci. *25*, 1052–1053.

429 34. Liu, Z.C., Liu, D.X., Chen, C., Li, D., Yang, A.J., Rong, M.Z., Chen, H.L., and Kong, M.G. (2015).
430 Physicochemical processes in the indirect interaction between surface air plasma and deionized water.
431 J. Phys. D: Appl. Phys. *48*, 495201.

432 35. Ledo, A., Fernandes, E., Salvador, A., Laranjinha, J., and Barbosa, R.M. (2022). In vivo hydrogen
433 peroxide diffusivity in brain tissue supports volume signaling activity. Redox Biol. *50*, 102250.

434 36. Tjell, A.Ø., and Almdal, K. (2018). Diffusion rate of hydrogen peroxide through water-swelled
435 polyurethane membranes. Sens. Bio-Sens. Res. *21*, 35–39.

436 37. Zandalinas, S.I., Fichman, Y., and Mittler, R. (2020). Vascular bundles mediate systemic reactive
437 oxygen signaling during light stress. Plant Cell *32*, 3425–3435.

438 38. Zandalinas, S.I., and Mittler, R. (2021). Vascular and nonvascular transmission of systemic reactive
439 oxygen signals during wounding and heat stress. Plant Physiol. *186*, 1721–1733.

440 39. Fürst-Jansen, J.M.R., de Vries, S., and de Vries, J. (2020). Evo-physio: on stress responses and the
441 earliest land plants. J. Exp. Bot. *71*, 3254–3269.

442 40. Hansel, C.M., and Diaz, J.M. (2021). Production of extracellular reactive oxygen species by marine
443 biota. Ann. Rev. Mar. Sci. *13*, 177–200.

444 41. Kawahara, T., Quinn, M.T., and Lambeth, J.D. (2007). Molecular evolution of the reactive oxygen-
445 generating NADPH oxidase (Nox/Duox) family of enzymes. BMC Evol. Biol. *7*, 109.

446 42. Lardy, B., Bof, M., Aubry, L., Paclet, M.H., Morel, F., Satre, M., and Klein, G. (2005). NADPH
447 oxidase homologs are required for normal cell differentiation and morphogenesis in Dictyostelium
448 discoideum. Biochim. Biophys. Acta *1744*, 199–212.

449 43. Aguirre, J., and Lambeth, J.D. (2010). Nox enzymes from fungus to fly to fish and what they tell us
450 about Nox function in mammals. Free Radic. Biol. Med. *49*, 1342–1353.

451 44. Ortega-Villasante, C., Burén, S., Barón-Sola, Á., Martínez, F., and Hernández, L.E. (2016). In vivo
452 ROS and redox potential fluorescent detection in plants: Present approaches and future perspectives.
453 Methods *109*, 92–104.

454 45. Lauffenburger, D.A., and Horwitz, A.F. (1996). Cell migration: a physically integrated molecular
455 process. Cell *84*, 359–369.

456 46. Smirnoff, N., and Arnaud, D. (2019). Hydrogen peroxide metabolism and functions in plants. New
457 Phytol. *221*, 1197–1214.

458 47. Sies, H., and Jones, D.P. (2020). Reactive oxygen species (ROS) as pleiotropic physiological signalling
459 agents. Nat. Rev. Mol. Cell Biol. *21*, 363–383.

460 48. Mittler, R., Zandalinas, S.I., Fichman, Y., and Van Breusegem, F. (2022). Reactive oxygen species
461 signalling in plant stress responses. Nat. Rev. Mol. Cell Biol., 10.1038/s41580-022-00499–2.

462 49. Čáp, M., Váchová, L., and Palková, Z. (2012). Reactive Oxygen Species in the signaling and adaptation
463 of multicellular microbial communities. Oxid. Med. Cell. Longev. *2012*, e976753.

464 50. Zheng, H., Kim, J., Liew, M., Yan, J.K., Herrera, O., Bok, J.W., Kelleher, N.L., Keller, N.P., and
465 Wang, Y. (2015). Redox metabolites signal Polymicrobial biofilm development via the NapA oxidative
466 stress cascade in Aspergillus. Curr. Biol. *25*, 29–37.

467 51. Sukenik, A., and Kaplan, A. (2021). Cyanobacterial harmful algal blooms in aquatic ecosystems: A
468 comprehensive outlook on current and emerging mitigation and control approaches. Microorganisms
469 *9*, 1472.

470 52. Martínez-Navarro, F.J., Martínez-Morcillo, F.J., de Oliveira, S., Candel, S., Cabas, I., García-Ayala,
471 A., Martínez-Menchón, T., Corbalán-Vélez, R., Mesa-Del-Castillo, P., Cayuela, M.L., et al. (2020).
472 Hydrogen peroxide in neutrophil inflammation: Lesson from the zebrafish. Dev. Comp. Immunol. *105*,
473 103583.

474 53. Iwashita, H., Castillo, E., Messina, M.S., Swanson, R.A., and Chang, C.J. (2021). A tandem activity-
475 based sensing and labeling strategy enables imaging of transcellular hydrogen peroxide signaling. Proc.
476 Natl. Acad. Sci. U.S.A. *118*, e2018513118.

477 54. Kuznetsov, A.V., Javadov, S., Saks, V., Margreiter, R., and Grimm, M. (2017). Synchronism in
478 mitochondrial ROS flashes, membrane depolarization and calcium sparks in human carcinoma cells.
479 Biochim. Biophys. Acta Bioenerg. *1858*, 418–431.

480 55. Chen, W., Luo, S., Xie, P., Hou, T., Yu, T., and Fu, X. (2018). Overexpressed UCP2 regulates
481 mitochondrial flashes and reverses lipopolysaccharide-induced cardiomyocytes injury. Am. J. Transl.
482 Res. *10*, 1347–1356.

483 56. Buvelot, H., Jaquet, V., and Krause, K.-H. (2019). Mammalian NADPH oxidases. In NADPH
484 Oxidases: Methods and Protocols Methods in Molecular Biology., U. G. Knaus and T. L. Leto, eds.
485 (Humana Press), pp. 17–36.

486 57. Liang, D. (2018). A salutary role of reactive oxygen species in intercellular tunnel-mediated
487 communication. Front. Cell. Dev. Biol. *6*, 2.

488 58. Xing, F., Hu, Q., Qin, Y., Xu, J., Zhang, B., Yu, X., and Wang, W. (2022). The relationship of redox
489 with hallmarks of cancer: The importance of homeostasis and context. Front. Oncol. *12*, 862743.

490 59. Liao, Z., Chua, D., and Tan, N.S. (2019). Reactive oxygen species: a volatile driver of field
491 cancerization and metastasis. Mol. Cancer *18*, 65.

492 60. Tsutsui, H., Kinugawa, S., and Matsushima, S. (2011). Oxidative stress and heart failure. Am. J.
493 Physiol. Heart Circ. Physiol. *301*, H2181–H2190.

494 61. Cadenas, S. (2018). ROS and redox signaling in myocardial ischemia-reperfusion injury and
495 cardioprotection. Free Radic. Biol. Med. *117*, 76–89.

496 62. Bugger, H., and Pfeil, K. (2020). Mitochondrial ROS in myocardial ischemia reperfusion and
497 remodeling. Biochim. Biophys. Acta Mol. Basis Dis. *1866*, 165768.

498 63. Fichman, Y., and Mittler, R. (2021). A systemic whole-plant change in redox levels accompanies the
499 rapid systemic response to wounding. Plant Physiol. *186*, 4–8.

500 64. Murashige, T., and Skoog, F. (1962). A revised medium for rapid growth and bio assays with tobacco
501 tissue cultures. Physiol. Plant. *15*, 473–497.

502 65. Gunadi, A., Li, F.-W., and Van Eck, J. (2022). Accelerating gametophytic growth in the model
503 hornwort Anthoceros agrestis. Appl. Plant Sci. *10*, e11460.

504 66. Cove, D.J., Perroud, P.-F., Charron, A.J., McDaniel, S.F., Khandelwal, A., and Quatrano, R.S. (2009).
505 The Moss Physcomitrella patens: A Novel model System for plant development and genomic studies.
506 Cold Spring Harb. Protoc. *2009*, pdb.emo115.

507 67. Hope, A.B., and Walker, N.A. (1975). The Physiology of Giant Algal Cells (Cambridge University
508 Press).

509 68. Froquet, R., Lelong, E., Marchetti, A., and Cosson, P. (2009). Dictyostelium discoideum: a model host
510 to measure bacterial virulence. Nat. Protoc. *4*, 25–30.

511 69. Sohn, Y.-S., Tamir, S., Song, L., Michaeli, D., Matouk, I., Conlan, A.R., Harir, Y., Holt, S.H., Shulaev,
512 V., Paddock, M.L., et al. (2013). NAF-1 and mitoNEET are central to human breast cancer proliferation
513 by maintaining mitochondrial homeostasis and promoting tumor growth. Proc. Natl. Acad. Sci. U.S.A.
514 *110*, 14676–14681.

515 70. Karmi, O., Holt, S.H., Song, L., Tamir, S., Luo, Y., Bai, F., Adenwalla, A., Darash-Yahana, M., Sohn,
516 Y.-S., Jennings, P.A., et al. (2017). Interactions between mitoNEET and NAF-1 in cells. PLoS One *12*,
517 e0175796.

518

519

520 **Figure legends**

521 **Figure 1.** ROS as rapid systemic signals in *Pinus sylvestris*, *Azolla filiculoides*, and *Selaginella*
522 *moellendorffii.* **(A)** *Pinus sylvestris* plants were subjected to a high light (HL) stress treatment applied to a
523 single leaf, and ROS accumulation was imaged, using H_2DCFDA, in whole plants (local and systemic
524 tissues, indicated with solid and dashed circles, respectively). Representative time-lapse images of whole
525 plant ROS accumulation in treated and untreated *Pinus sylvestris* plants are shown alongside bar graphs of
526 combined data from all plants used for the analysis at the 0- and 30-min time points (local and systemic).
527 **(B)** Same as A but for *Azolla filiculoides*. **(C)** Same as A, but for *Selaginella moellendorffii*. All experiments
528 were repeated at least 3 times with 10 plants per experiment. Data is presented as box plot graphs; X is
529 mean ± S.E., N=30, *P < 0.05, **P < 0.01, Student t-test. Scale bar, 1 cm. Abbreviations: H_2DCFDA, 2',7'-
530 dichlorodihydrofluorescein diacetate; HL, high light; L, local; ROS, reactive oxygen species; S, systemic.

531 **Figure 2.** Rapid systemic ROS signaling in non-vascular plants. **(A)** *Anthoceros agrestis* plants were
532 subjected to a high light (HL) stress treatment applied to a single leaf and ROS accumulation was imaged
533 using H_2DCFDA, in whole plants (local and systemic tissues, indicated with solid and dashed circles,
534 respectively). Representative time-lapse images of whole plant ROS accumulation in treated and untreated
535 *Anthoceros agrestis* plants are shown alongside bar graphs of combined data from all plants used for the
536 analysis at the 0- and 30-min time points (local and systemic). **(B)** Same as A but for *Marchantia*
537 *polymorpha*. **(C)** Same as A, but for *Physcomitrium patens*. All experiments were repeated at least 3 times
538 with 10 plants per experiment. Data is presented as box plot graphs; X is mean ± S.E., N=30, *P < 0.05,
539 **P < 0.01, ***P < 0.001, Student t-test. Scale bar, 1 cm. Abbreviations: H_2DCFDA, 2',7'-
540 dichlorodihydrofluorescein diacetate; HL, high light; L, local; ROS, reactive oxygen species; S, systemic.

541 **Figure 3.** Rapid systemic ROS signaling in multicellular algae and unicellular organisms. **(A)** *Chara*
542 *vulgaris*, a multicellular alga, was subjected to a high light (HL) stress treatment applied to a single branch,
543 and ROS accumulation was imaged, using H_2DCFDA, in several branches of the alga (local and systemic
544 tissues, indicated with solid and dashed circles, respectively). Representative time-lapse images of whole
545 alga ROS accumulation in treated and untreated *Chara vulgaris* are shown alongside bar graphs of
546 combined data from all plants used for the analysis at the 0- and 30-min time points (local and systemic).
547 **(B)** An agar plate containing a lawn of *Chlamydomonas reinhardtii*, a unicellular alga, was treated with a
548 focused beam of HL (local treatment), and ROS accumulation was imaged, using H_2DCFDA, in the entire
549 plate (local and systemic tissues are indicated with solid and dashed circles, respectively). Representative
550 time-lapse images of whole plate ROS accumulation of treated and untreated *Chlamydomonas* lawn are
551 shown alongside bar graphs of combined data from all plants used for the analysis at the 0- and 30-min time
552 points (local and systemic). **(C)** Same as in B, but for an agar plate that contains a lawn of *Dictyostelium*

553 *discoideum* that was treated locally with a heated rod (local). All experiments were repeated at least 3 times
554 with 10 multicellular alga, or agar plates per experiment. Data is presented as box plot graphs; X is mean ±
555 S.E., N=30, *P < 0.05, **P < 0.01, ***P < 0.001, Student t-test. Scale bar, 1 cm. Abbreviations: H_2DCFDA,
556 2',7'-dichlorodihydrofluorescein diacetate; HL, high light; L, local; ROS, reactive oxygen species; S,
557 systemic.

558 **Figure 4.** Activation of the rapid systemic ROS signal in *Physcomitrium patens*, *Chlamydomonas*
559 *reinhardtii*, and *Dictyostelium discoideum* by a local application of H_2O_2. **(A)** An agar plate without
560 *Physcomitrium patens* (top), and agar plates with a lawn of *Physcomitrium patens* (middle and bottom),
561 were treated with 1 ul of 1 mM H_20_2 (top and bottom), or 1 ul of media (mock, middle), and ROS
562 accumulation was imaged using H_2DCFDA in the entire plate. Representative time-lapse images of whole
563 plate ROS accumulation are shown alongside bar graphs of combined data from all plates used for the
564 analysis at the 0- and 30-min time points (local and systemic). Local and systemic sampling locations are
565 indicated with solid and dashed circles, respectively. **(B)** Same as A, but for plates with or without a lawn
566 of *Chlamydomonas reinhardtii*. **(C)** Same as in A, but for plates with or without *Dictyostelium discoideum*.
567 All experiments were repeated at least 3 times with 10 agar plates per experiment. Data is presented as box
568 plot graphs; X is mean ± S.E., N=30, *P < 0.05, **P < 0.01, ***P < 0.001, Student t-test. Scale bar, 1 cm.
569 Abbreviations: H_2DCFDA, 2',7'-dichlorodihydrofluorescein diacetate; HL, high light; L, local; ROS,
570 reactive oxygen species; S, systemic.

571 **Figure 5.** Inhibition of the rapid systemic ROS signal in *Physcomitrium patens*, *Chlamydomonas*
572 *reinhardtii*, and *Dictyostelium discoideum* by DPI. **(A)** A diagram showing the experimental design used.
573 A strip of agar containing water or the NOX/RBOH inhibitor DPI (50 μM) was layered over the middle of
574 agar plates containing a lawn of the different organisms growing on them. Following a 5 min incubation
575 one side of the plate was treated with a focused beam of high light (HL) or touched with a heated rod (local)
576 and ROS accumulation was imaged using H_2DCFDA in the entire plate. Local and systemic locations used
577 for signal quantification are indicated with solid and dashed circles, respectively. **(B)** Representative time-
578 lapse images of whole plate ROS accumulation are shown alongside bar graphs of combined data from all
579 plates used for the analysis at the 0- and 30-min time points (Water or DPI treated *Physcomitrium patens*,
580 *Chlamydomonas reinhardtii*, or *Dictyostelium discoideum*; top, middle, and bottom, respectively; local and
581 systemic). All experiments were repeated at least 3 times with 10 agar plates per experiment. Data is
582 presented as box plot graphs; X is mean ± S.E., N=30, **P < 0.01, ***P < 0.001, Student t-test. Scale bar,
583 1 cm. Abbreviations: DPI, diphenyleneiodonium; H_2DCFDA, 2',7'-dichlorodihydrofluorescein diacetate;
584 HL, high light; L, local; NOX, NADPH oxidase; RBOH, respiratory burst oxidase homolog; ROS, reactive
585 oxygen species; S, systemic.

586 **Figure 6.** Functional analysis of the cell-to-cell rapid ROS signal in *Chlamydomonas reinhardtii*. **(A)**
587 Diagrams showing the experimental designs used. Left: A lawn of *Chlamydomonas reinhardtii* growing on
588 an agar plate was subjected to a focused beam of high light (HL) stress and the area subjected to the beam
589 (local, L), as well as an area that is on the other end of the plate (systemic, S) were sampled at different
590 times following the application of HL for analysis of the expression of the light stress response small heat
591 shock protein 17.1 (sHSP17.1; This design was used for the experiments shown in B). Right: A strip of
592 agar containing water or the NOX/RBOH inhibitor DPI (50 μM) was layered over the middle of agar plates
593 containing the lawn of *Chlamydomonas reinhardtii* 5 min prior to the application of light stress and
594 sampling (This design was used for the experiments shown in C). Local and systemic sampling locations
595 are indicated with solid and dashed circles, respectively. **(B)** Representative protein blots and Coomassie-
596 stained gels are shown alongside bar graphs of combined data from all blots used for the analysis at the 0-,
597 2-, and 30-min time points, for the expression of sHSP17.1 in the L and S locations, following the light
598 stress treatment. **(C)** Same as in B, but for experiments in which a strip of agar containing water (left) or
599 DPI (right) was layered over the middle of agar plates 5 min prior to the application of HL stress. All
600 experiments were repeated at least 3 times with 10 agar plates per experiment. Data is presented as box plot
601 graphs; X is mean ± S.E., N=30, *P < 0.05, **P < 0.01, ***P < 0.001, Student t-test. Scale bar, 1 cm.
602 Abbreviations: DPI, diphenyleneiodonium; H_2DCFDA, 2',7'-dichlorodihydrofluorescein diacetate; HL,
603 high light; L, local; NOX, NADPH oxidase; RBOH, respiratory burst oxidase homolog; ROS, reactive
604 oxygen species; S, systemic; sHSP, small heat shock protein 17.1.

605 **Figure 7.** Rapid systemic ROS signaling in mammalian cells. **(A)** Monolayers of human epithelial breast
606 cancer (MDA-MB-231; top), and rat cardiomyocytes (H9c2; bottom), cells grown in culture were treated
607 with a heated metal rod to induce injury (average injury diameter is 120 μm) and ROS accumulation was
608 imaged using H_2DCFDA in the entire plate. Representative time-lapse images of whole plate ROS
609 accumulation in treated and untreated plates are shown alongside bar graphs of combined data from all
610 plates used for the analysis at the 0- and 30-min time points (local and systemic). Local and systemic
611 sampling locations are indicated with solid and dashed circles, respectively. **(B)** Same as in A, except that
612 buffer or DPI (50 μM) were added to the growth media of cells 10 min prior to the heat injury. All
613 experiments were repeated at least 3 times with 10 agar plates per experiment. Data is presented as box plot
614 graphs; X is mean ± S.E., N=30, **P < 0.01, ***P < 0.001, Student t-test. Scale bar, 1 cm. Abbreviations:
615 DPI, diphenyleneiodonium; H_2DCFDA, 2',7'-dichlorodihydrofluorescein diacetate; L, local; ROS, reactive
616 oxygen species; S, systemic.

617 **Figure 8.** A model depicting the principle of the cell-to-cell ROS signaling pathway that is conserved
618 between unicellular and multicellular organisms. An initiating cell that perceives a stress or ROS signal is

619 shown on the left to undergo a change in redox levels that will cause the accumulation of ROS in that cell.
620 This process is shown to cause the activation of a paracrine and juxtacrine ROS-mediated cell-to-cell signal
621 transduction pathway. Each cell along the path of this pathway accumulates ROS maintaining the signal
622 and transmitting it to the next. The resulting changes in redox in all cells involved in this signaling pathway
623 activate gene expression via oxidative post translational modification (oxi-PTM) of different regulatory
624 proteins, yielding a coordinated cellular response to the original stress or signal in the entire colony, biofilm,
625 and/or tissue. Please see text for more details. Abbreviations: oxi-PTM, oxidative post translational
626 modification; ROS, reactive oxygen species.

627 **Figure S1.** Controls for the detection of H_2O_2 on agar plates (in support of Figure 4). Agar plates containing
628 the different growth media used in Figure 4, but without any organisms growing on them, were fumigated
629 with OxyBurst, which detects ROS in the absence of cells. A 1 µL drop of 10 mM or 1 M H_2O_2 was then
630 applied to the plate (indicated with a circle) and whole plate ROS accumulation was imaged for 30 min.
631 Scale bar, 1 cm.

632 **Figure S2.** Representative images of injury inflicted on the H9c2 cell monolayer by a heat-treated metal
633 rod (in support of Figure 7A). Plates with a monolayer of H9c2 cells, used for the experiments shown in
634 Figure 7A were imaged with an Agilent BioTek Lionheart FX automated microscope and the different
635 images collected were assembled to reveal the size of injury inflicted on the monolayer of cells. Scale bar,
636 200 µM.

637 **Figure S3.** Controls for the ability of H9c2 cells that do not show ROS accumulation following the heated
638 rod injury to accumulate ROS (in support of Figure 7). Monolayers of rat cardiomyocytes (H9c2), cells
639 grown in culture were treated or untreated with a heated metal rod (indicated with a circle) to induce injury
640 (average injury diameter is 120 µm) and ROS accumulation was imaged using H_2DCFDA for 60 min in the
641 entire plate. At the end of the 60 min, H_2O_2 at a final concentration of 1 mM was added to the plates and
642 the plates were imaged for an additional 10 min. Representative time-lapse images of whole plate ROS
643 accumulation in treated and untreated plates are shown. Scale bar, 1 cm. Abbreviations: H_2DCFDA, 2',7'-
644 dichlorodihydrofluorescein diacetate; ROS, reactive oxygen species.

645 **Movie S1.** A movie showing the ROS signal generated in a monolayer of H9c2 cells following heat injury
646 (in support of Figure 7A). Monolayers of rat cardiomyocytes (H9c2) cells grown in culture were treated
647 with a heated metal rod (indicated with a circle) to induce injury (average injury diameter is 120 µm) and
648 ROS accumulation was imaged using H_2DCFDA in the entire plate. Abbreviations: H_2DCFDA, 2',7'-
649 dichlorodihydrofluorescein diacetate.

650

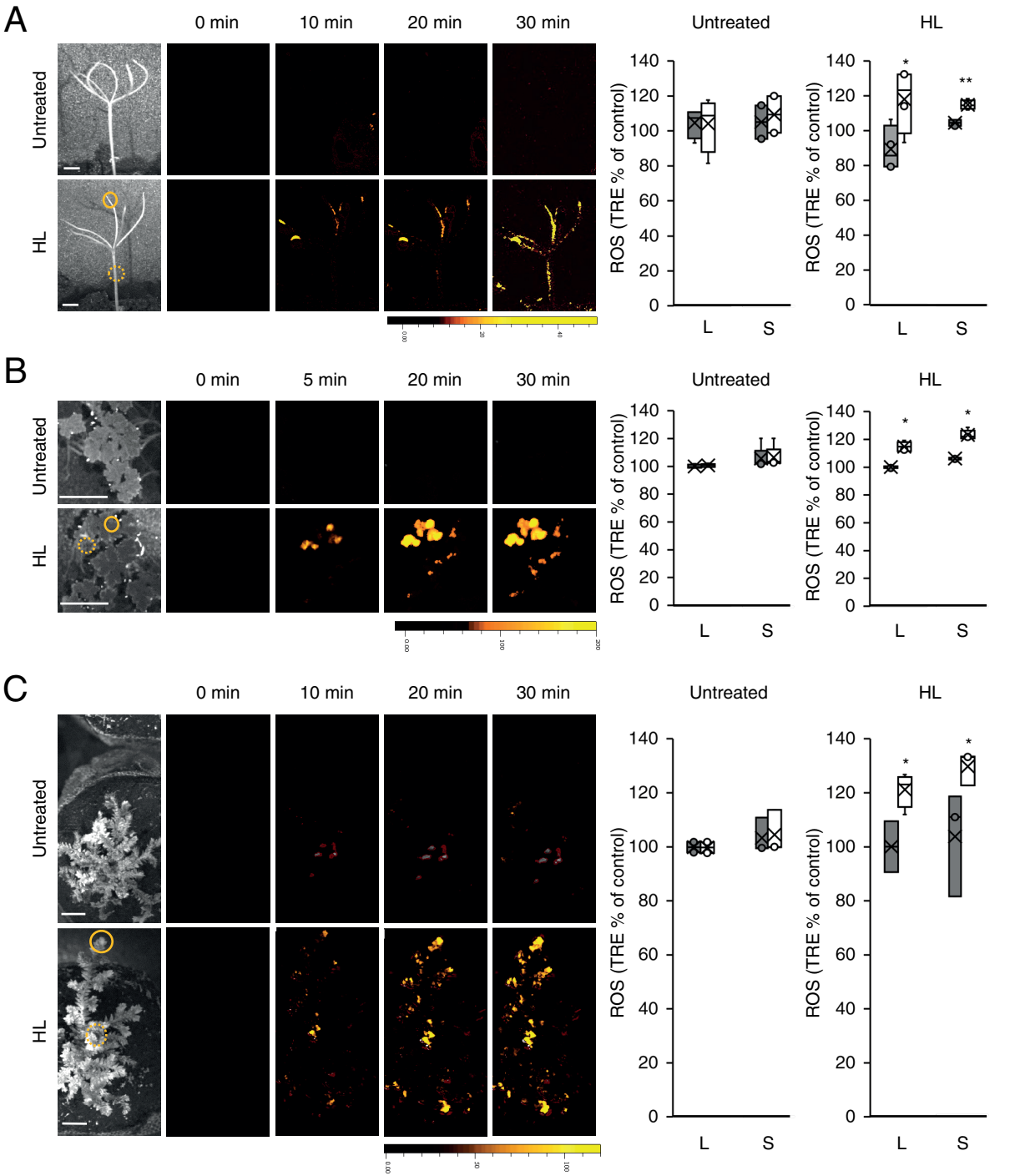

Figure 1. ROS as rapid systemic signals in *Pinus sylvestris*, *Azolla filiculoides*, and *Selaginella moellendorffii.* **(A)** *Pinus sylvestris* plants were subjected to a high light (HL) stress treatment applied to a single leaf, and ROS accumulation was imaged, using H_2DCFDA, in whole plants (local and systemic tissues, indicated with solid and dashed circles, respectively). Representative time-lapse images of whole plant ROS accumulation in treated and untreated *Pinus sylvestris* plants are shown alongside bar graphs of combined data from all plants used for the analysis at the 0- and 30-min time points (local and systemic). **(B)** Same as A but for *Azolla filiculoides*. **(C)** Same as A, but for *Selaginella moellendorffii*. All experiments were repeated at least 3 times with 10 plants per experiment. Data is presented as box plot graphs; X is mean ± S.E., N=30, *P < 0.05, **P < 0.01, Student t-test. Scale bar, 1 cm. Abbreviations: H_2DCFDA, 2',7'-dichlorodihydrofluorescein diacetate; HL, high light; L, local; ROS, reactive oxygen species; S, systemic.

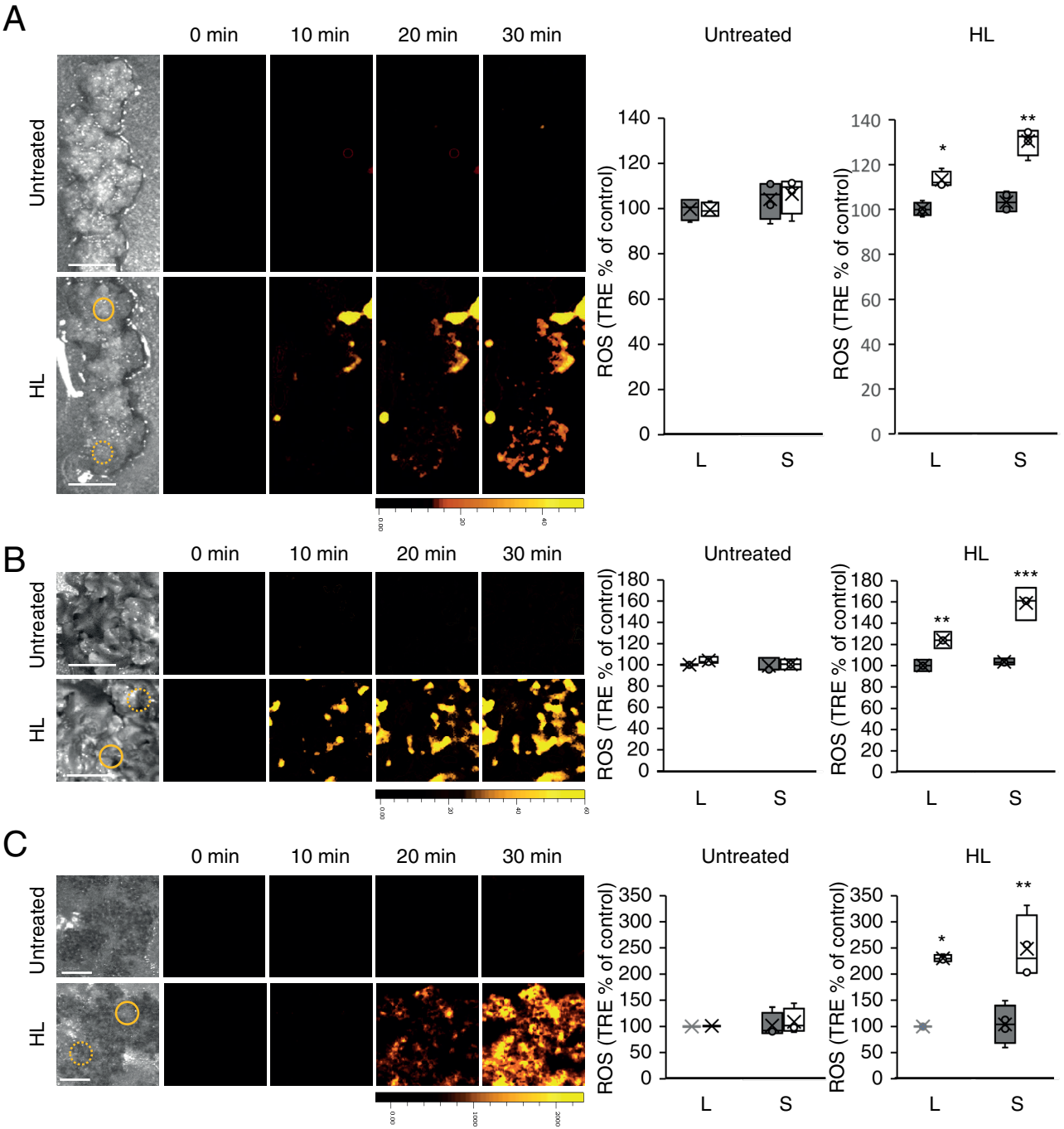

Figure 2. Rapid systemic ROS signaling in non-vascular plants. **(A)** *Anthoceros agrestis* plants were subjected to a high light (HL) stress treatment applied to a single leaf and ROS accumulation was imaged using H_2DCFDA, in whole plants (local and systemic tissues, indicated with solid and dashed circles, respectively). Representative time-lapse images of whole plant ROS accumulation in treated and untreated *Anthoceros agrestis* plants are shown alongside bar graphs of combined data from all plants used for the analysis at the 0- and 30-min time points (local and systemic). **(B)** Same as A but for *Marchantia polymorpha*. **(C)** Same as A, but for *Physcomitrium patens*. All experiments were repeated at least 3 times with 10 plants per experiment. Data is presented as box plot graphs; X is mean ± S.E., N=30, *P < 0.05, **P < 0.01, ***P < 0.001, Student t-test. Scale bar, 1 cm. Abbreviations: H_2DCFDA, 2',7'-dichlorodihydrofluorescein diacetate; HL, high light; L, local; ROS, reactive oxygen species; S, systemic.

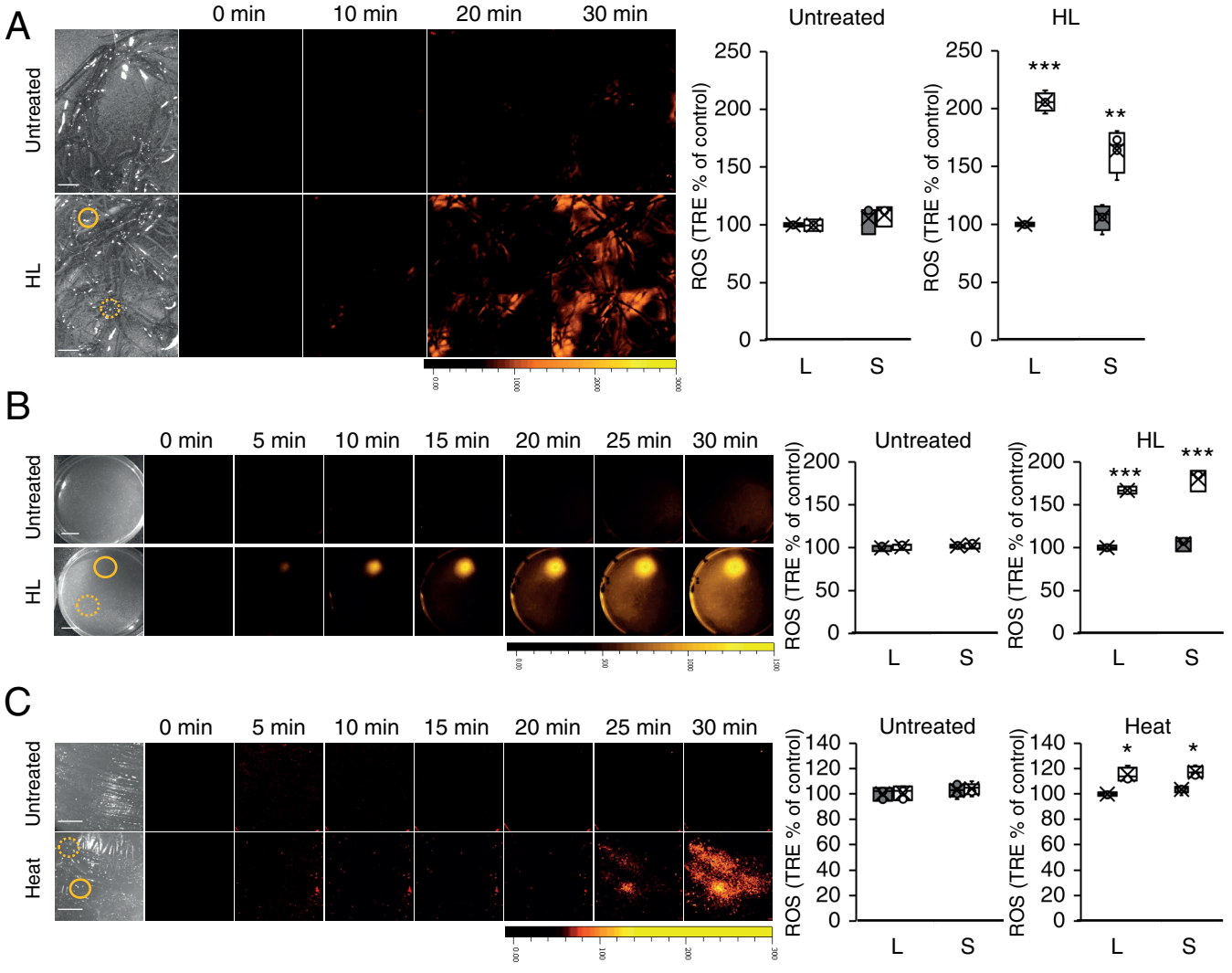

Figure 3. Rapid systemic ROS signaling in multicellular algae and unicellular organisms. **(A)** *Chara vulgaris*, a multicellular alga, was subjected to a high light (HL) stress treatment applied to a single branch, and ROS accumulation was imaged, using H_2DCFDA, in several branches of the alga (local and systemic tissues, indicated with solid and dashed circles, respectively). Representative time-lapse images of whole alga ROS accumulation in treated and untreated *Chara vulgaris* are shown alongside bar graphs of combined data from all plants used for the analysis at the 0- and 30-min time points (local and systemic). **(B)** An agar plate containing a lawn of *Chlamydomonas reinhardtii*, a unicellular alga, was treated with a focused beam of HL (local treatment), and ROS accumulation was imaged, using H_2DCFDA, in the entire plate (local and systemic tissues are indicated with solid and dashed circles, respectively). Representative time-lapse images of whole plate ROS accumulation of treated and untreated *Chlamydomonas* lawn are shown alongside bar graphs of combined data from all plants used for the analysis at the 0- and 30-min time points (local and systemic). **(C)** Same as in B, but for an agar plate that contains a lawn of *Dictyostelium discoideum* that was treated locally with a heated rod (local). All experiments were repeated at least 3 times with 10 multicellular alga, or agar plates per experiment. Data is presented as box plot graphs; $\bar{X}$ is mean ± S.E., N=30, *P < 0.05, **P < 0.01, ***P < 0.001, Student t-test. Scale bar, 1 cm. Abbreviations: H_2DCFDA, 2',7'-dichlorodihydrofluorescein diacetate; HL, high light; L, local; ROS, reactive oxygen species; S, systemic.

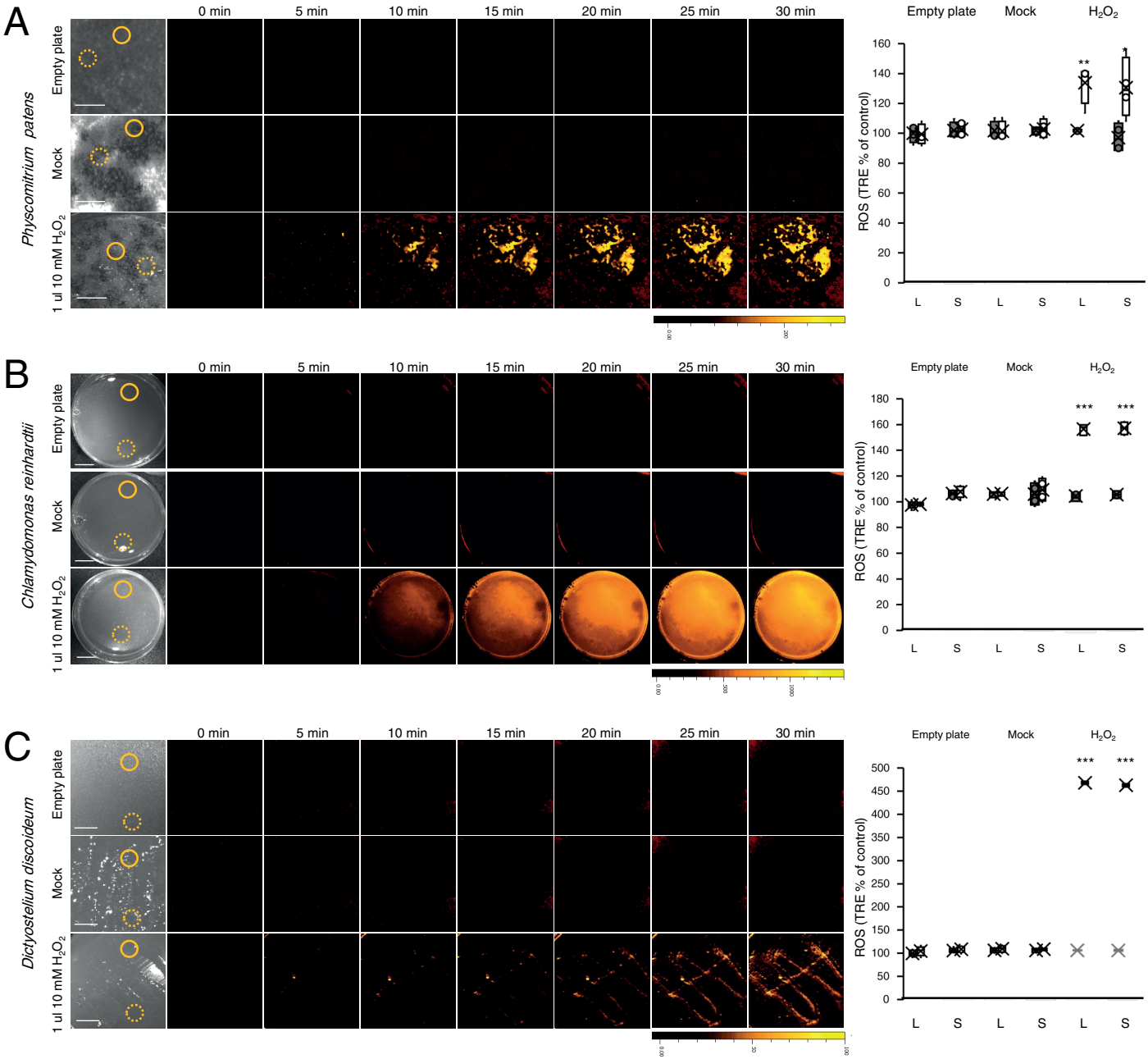

Figure 4. Activation of the rapid systemic ROS signal in *Physcomitrium patens*, *Chlamydomonas reinhardtii*, and *Dictyostelium discoideum* by a local application of H_2O_2. **(A)** An agar plate without *Physcomitrium patens* (top), and agar plates with a lawn of *Physcomitrium patens* (middle and bottom), were treated with 1 ul of 1 mM H_20_2 (top and bottom), or 1 ul of media (mock, middle), and ROS accumulation was imaged using H_2DCFDA in the entire plate. Representative time-lapse images of whole plate ROS accumulation are shown alongside bar graphs of combined data from all plates used for the analysis at the 0- and 30-min time points (local and systemic). Local and systemic sampling locations are indicated with solid and dashed circles, respectively. **(B)** Same as A, but for plates with or without a lawn of *Chlamydomonas reinhardtii*. **(C)** Same as in A, but for plates with or without *Dictyostelium discoideum*. All experiments were repeated at least 3 times with 10 agar plates per experiment. Data is presented as box plot graphs; X is mean ± S.E., N=30, *P < 0.05, **P < 0.01, ***P < 0.001, Student t-test. Scale bar, 1 cm. Abbreviations: H_2DCFDA, 2',7'-dichlorodihydrofluorescein diacetate; HL, high light; L, local; ROS, reactive oxygen species; S, systemic.

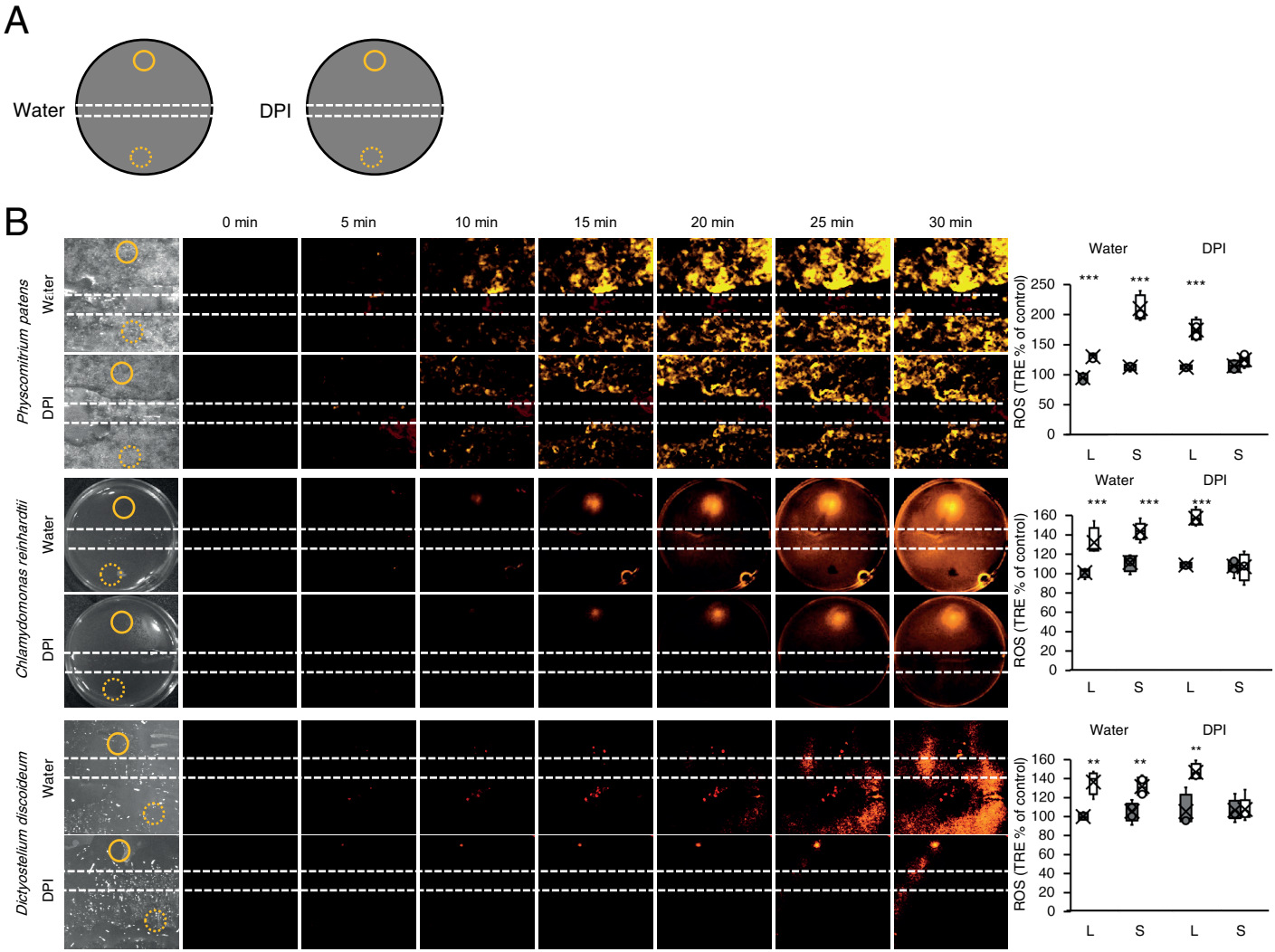

Figure 5. Inhibition of the rapid systemic ROS signal in *Physcomitrium patens*, *Chlamydomonas reinhardtii*, and *Dictyostelium discoideum* by DPI. **(A)** A diagram showing the experimental design used. A strip of agar containing water or the NOX/RBOH inhibitor DPI (50 µM) was layered over the middle of agar plates containing a lawn of the different organisms growing on them. Following a 5 min incubation one side of the plate was treated with a focused beam of high light (HL) or touched with a heated rod (local) and ROS accumulation was imaged using H_2DCFDA in the entire plate. Local and systemic locations used for signal quantification are indicated with solid and dashed circles, respectively. **(B)** Representative time-lapse images of whole plate ROS accumulation are shown alongside bar graphs of combined data from all plates used for the analysis at the 0- and 30-min time points (Water or DPI treated *Physcomitrium patens*, *Chlamydomonas reinhardtii*, or *Dictyostelium discoideum*; top, middle, and bottom, respectively; local and systemic). All experiments were repeated at least 3 times with 10 agar plates per experiment. Data is presented as box plot graphs; X is mean ± S.E., N=30, **P < 0.01, ***P < 0.001, Student t-test. Scale bar, 1 cm. Abbreviations: DPI, diphenyleneiodonium; H_2DCFDA, 2',7'-dichlorodihydrofluorescein diacetate; HL, high light; L, local; NOX, NADPH oxidase; RBOH, respiratory burst oxidase homolog; ROS, reactive oxygen species; S, systemic.

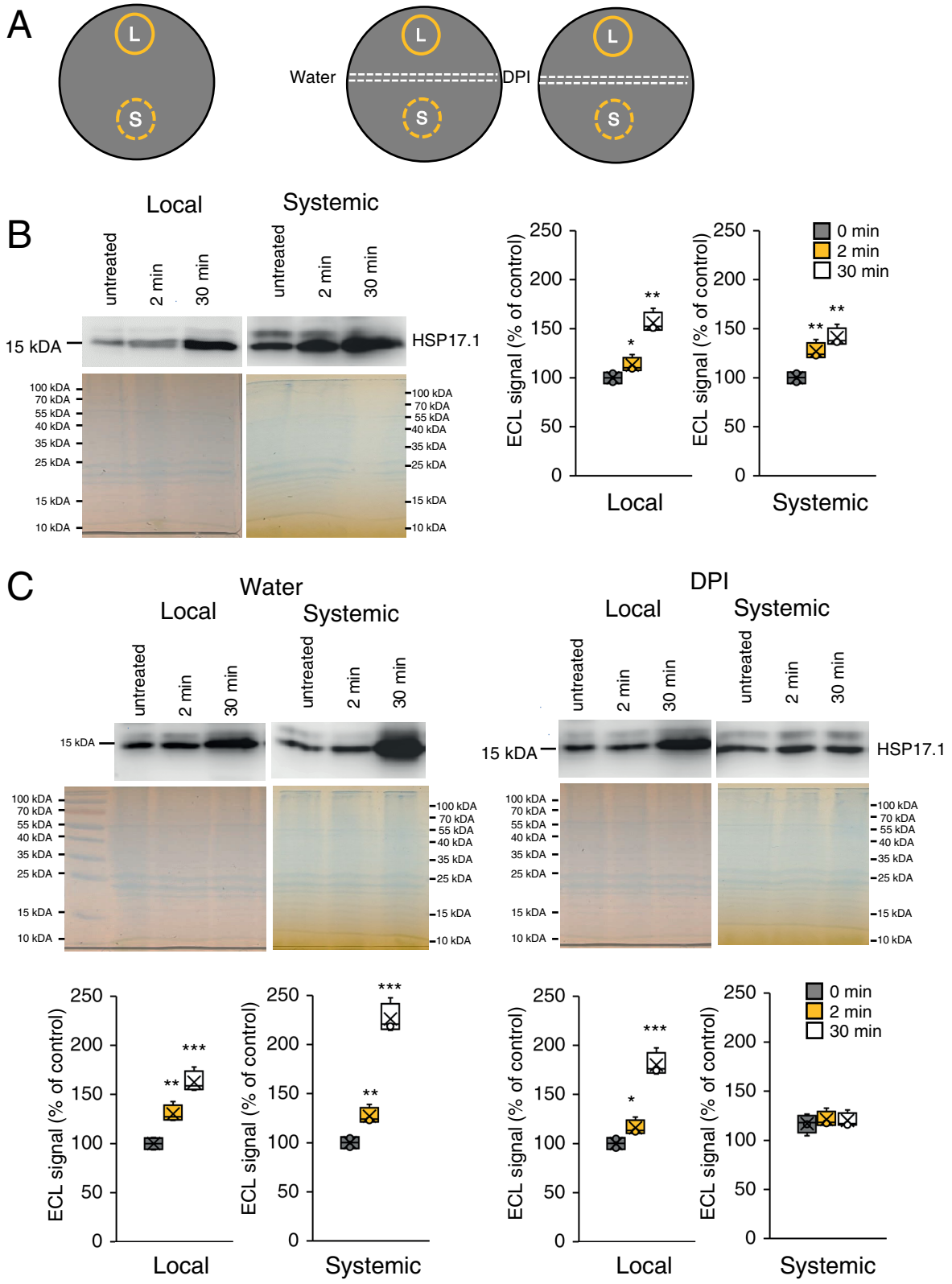

Figure 6. Functional analysis of the cell-to-cell rapid ROS signal in *Chlamydomonas reinhardtii*. **(A)** Diagrams showing the experimental designs used. Left: A lawn of *Chlamydomonas reinhardtii* growing on an agar plate was subjected to a focused beam of high light (HL) stress and the area subjected to the beam (local, L), as well as an area that is on the other end of the plate (systemic, S) were sampled at different times following the application of HL for analysis of the expression of the light stress response small heat shock protein 17.1 (sHSP17.1; This design was used for the experiments shown in B). Right: A strip of agar containing water or the NOX/RBOH inhibitor DPI (50 μM) was layered over the middle of agar plates containing the lawn of *Chlamydomonas reinhardtii* 5 min prior to the application of light stress and sampling (This design was used for the experiments shown in C). Local and systemic sampling locations are indicated with solid and dashed circles, respectively. **(B)** Representative protein blots and Coomassie- stained gels are shown alongside bar graphs of combined data from all blots used for the analysis at the 0-, 2-, and 30-min time points, for the expression of sHSP17.1 in the L and S locations, following the light stress treatment. **(C)** Same as in B, but for experiments in which a strip of agar containing water (left) or DPI (right) was layered over the middle of agar plates 5 min prior to the application of HL stress. All experiments were repeated at least 3 times with 10 agar plates per experiment. Data is presented as box plot graphs; X is mean ± S.E., N=30, *P < 0.05, **P < 0.01, ***P < 0.001, Student t-test. Abbreviations: DPI, diphenyleneiodonium; H_2DCFDA, 2',7'-dichlorodihydrofluorescein diacetate; HL, high light; L, local; NOX, NADPH oxidase; RBOH, respiratory burst oxidase homolog; ROS, reactive oxygen species; S, systemic; sHSP, small heat shock protein 17.1.

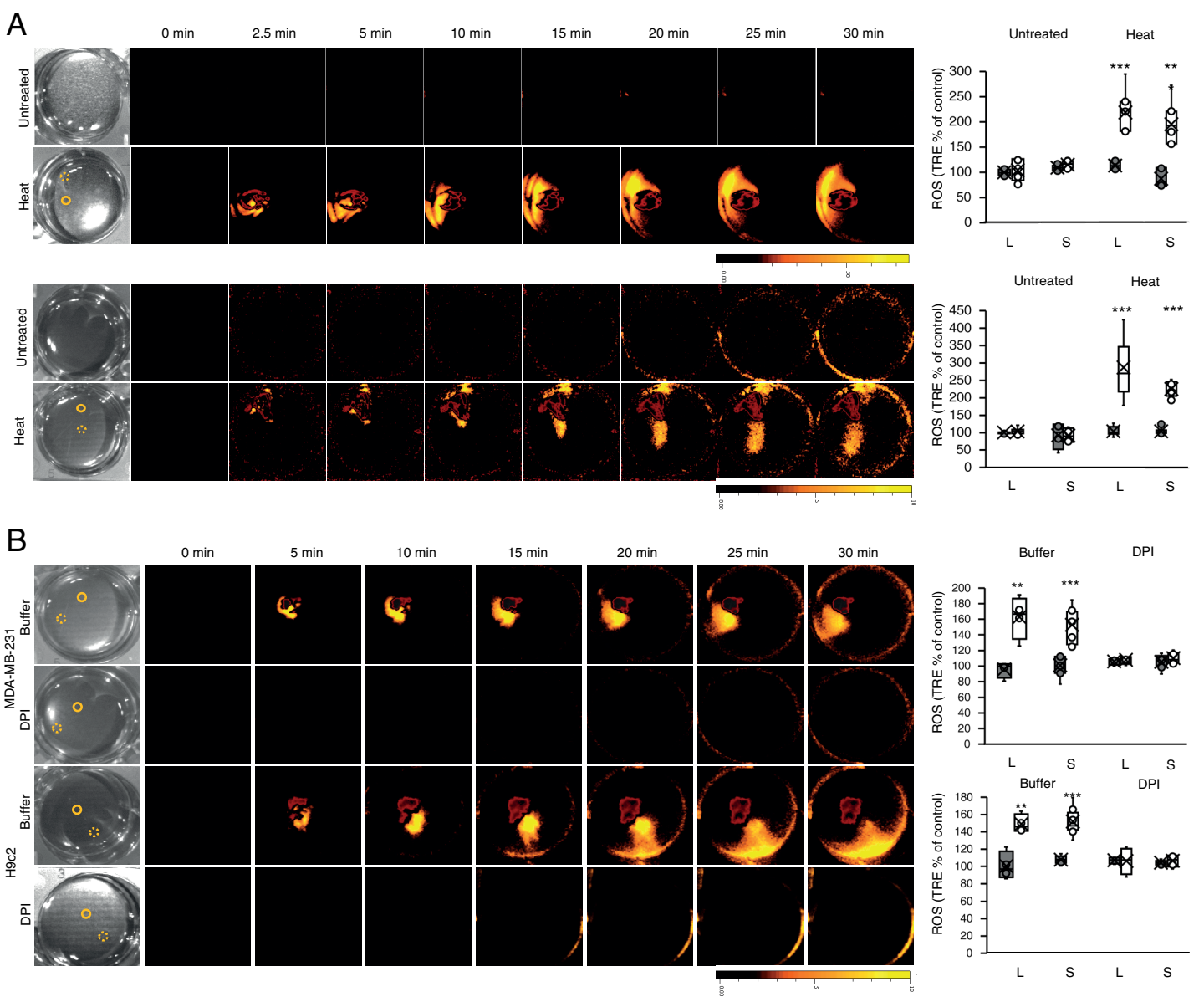

Figure 7. Rapid systemic ROS signaling in mammalian cells. **(A)** Monolayers of human epithelial breast cancer (MDA-MB-231; top), and rat cardiomyocytes (H9c2; bottom), cells grown in culture were treated with a heated metal rod to induce injury (average injury diameter is 120 µm) and ROS accumulation was imaged using H_2DCFDA in the entire plate. Representative time-lapse images of whole plate ROS accumulation in treated and untreated plates are shown alongside bar graphs of combined data from all plates used for the analysis at the 0- and 30-min time points (local and systemic). Local and systemic sampling locations are indicated with solid and dashed circles, respectively. **(B)** Same as in A, except that buffer or DPI (50 µM) were added to the growth media of cells 10 min prior to the heat injury. All experiments were repeated at least 3 times with 10 agar plates per experiment. Data is presented as box plot graphs; X is mean ± S.E., N=30, **P < 0.01, ***P < 0.001, Student t-test. Scale bar, 1 cm. Abbreviations: DPI, diphenyleneiodonium; H_2DCFDA, 2',7'-dichlorodihydrofluorescein diacetate; L, local; ROS, reactive oxygen species; S, systemic.

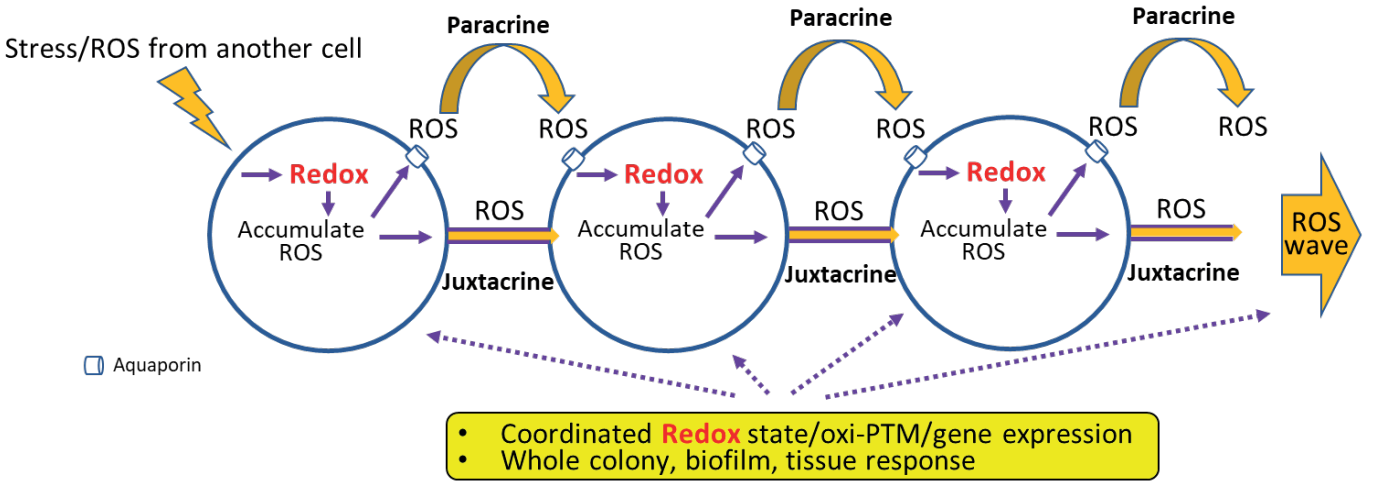

Figure 8. A model depicting the principle of the cell-to-cell ROS signaling pathway that is conserved between unicellular and multicellular organisms. An initiating cell that perceives a stress or ROS signal is shown on the left to undergo a change in redox levels that will cause the accumulation of ROS in that cell. This process is shown to cause the activation of a paracrine and juxtacrine ROS-mediated cell-to-cell signal transduction pathway. Each cell along the path of this pathway accumulates ROS maintaining the signal and transmitting it to the next. The resulting changes in redox in all cells involved in this signaling pathway activate gene expression via oxidative post translational modification (oxi-PTM) of different regulatory proteins, yielding a coordinated cellular response to the original stress or signal in the entire colony, biofilm, and/or tissue. Please see text for more details. Abbreviations: oxi-PTM, oxidative post translational modification; ROS, reactive oxygen species.

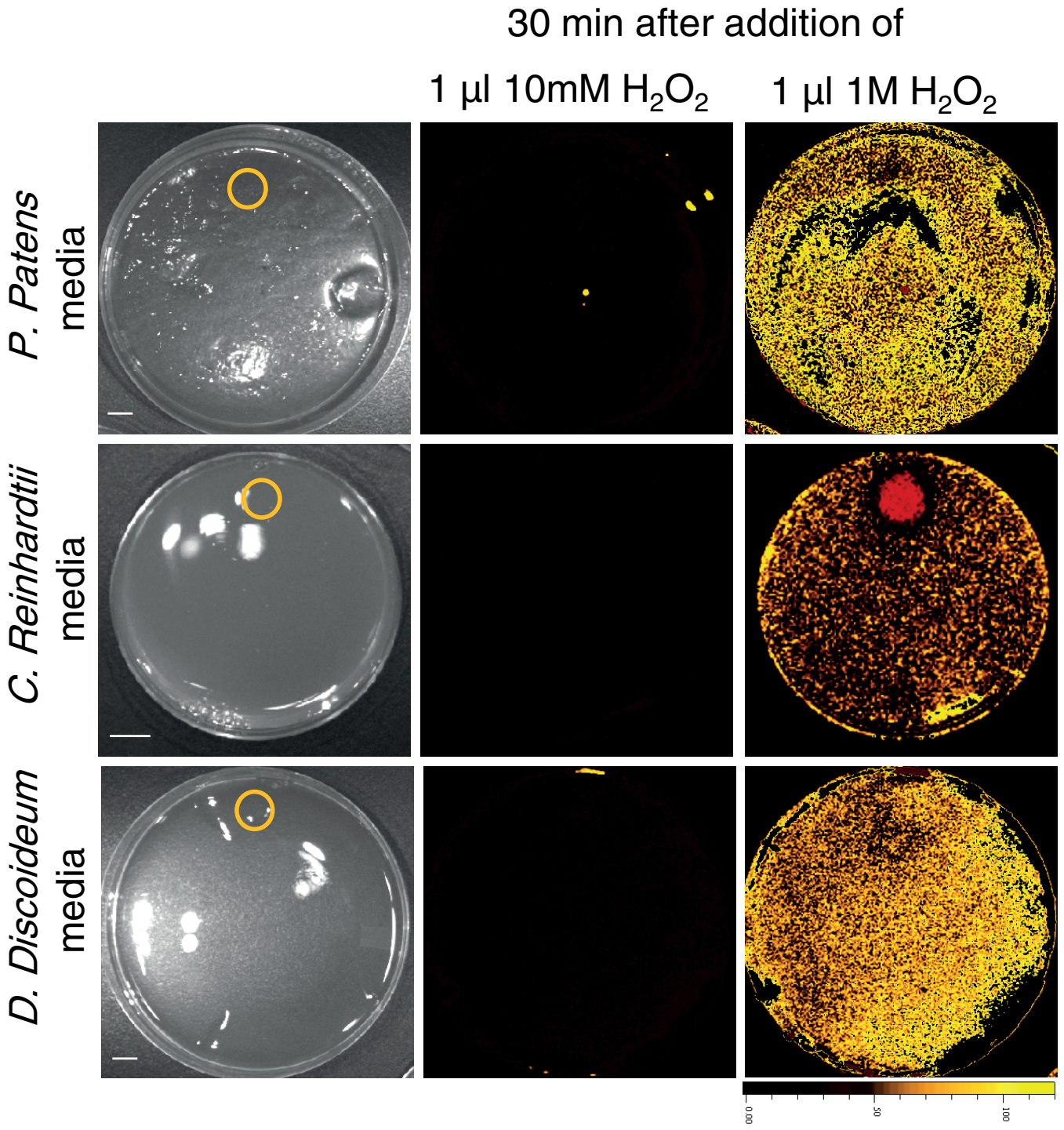

Figure S1. Controls for the detection of H_2O_2 on agar plates (in support of Figure 4). Agar plates containing the different growth media used in Figure 4, but without any organisms growing on them, were fumigated with OxyBurst, which detects ROS in the absence of cells. A 1 µL drop of 10 mM or 1 M H_2O_2 was then applied to the plate (indicated with a circle) and whole plate ROS accumulation was imaged for 30 min. Scale bar, 1 cm.

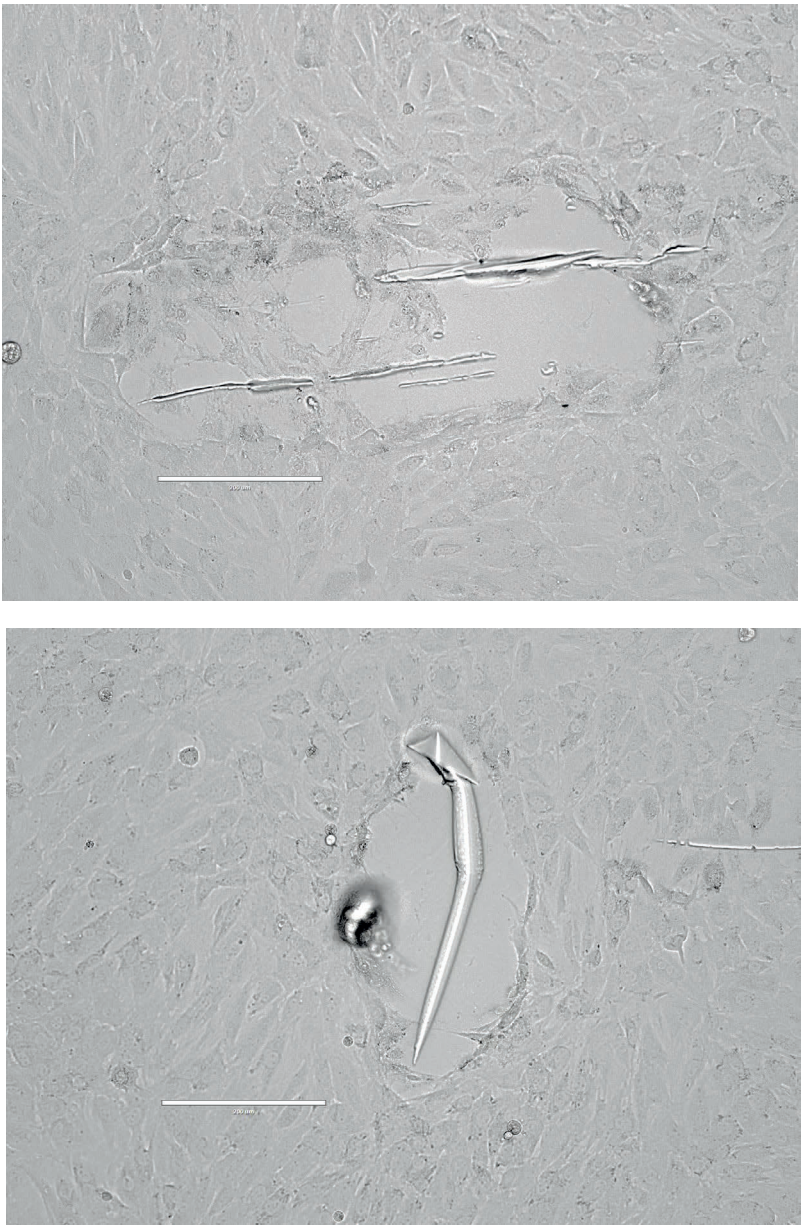

Figure S2. Representative images of injury inflicted on the H9c2 cell monolayer by a heat-treated metal rod (in support of Figure 7A). Plates with a monolayer of H9c2 cells, used for the experiments shown in Figure 7A were imaged with an Agilent BioTek Lionheart FX automated microscope and the different images collected were assembled to reveal the size of injury inflicted on the monolayer of cells. Scale bar, 200 µM.

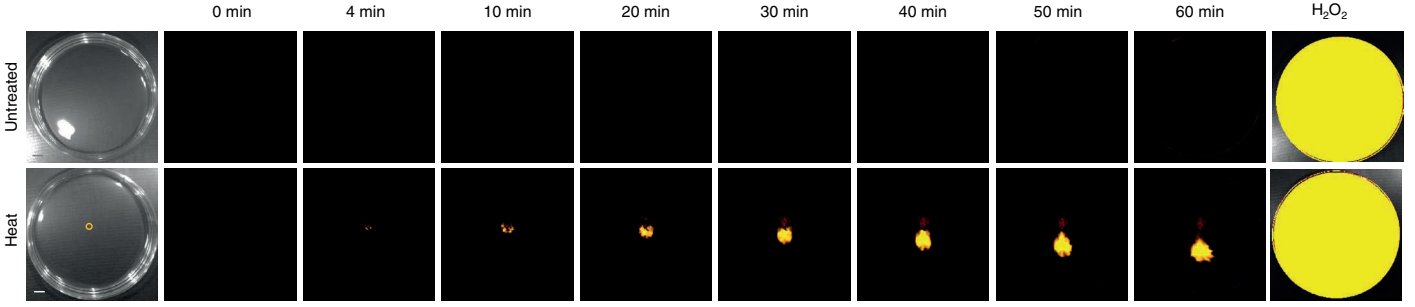

Figure S3. Controls for the ability of H9c2 cells that do not show ROS accumulation following the heated rod injury to accumulate ROS (in support of Figure 7). Monolayers of rat cardiomyocytes (H9c2), cells grown in culture were treated or untreated with a heated metal rod (indicated with a circle) to induce injury (average injury diameter is 120 µm) and ROS accumulation was imaged using H_2DCFDA for 60 min in the entire plate. At the end of the 60 min, H_2O_2 at a final concentration of 1 mM was added to the plates and the plates were imaged for an additional 10 min. Representative time-lapse images of whole plate ROS accumulation in treated and untreated plates are shown. Scale bar, 1 cm. Abbreviations: H_2DCFDA, 2',7'-dichlorodihydrofluorescein diacetate; ROS, reactive oxygen species.

Table S1 – Rates of the ROS wave in the different experiments

Figure	description	rate (cm min^{-1})	Treatment
1A	*Pinus sylvestris*	0.18	HL
1B	*Azolla filiculoides*	0.1	
1C	*Selaginella moellendorffii*	0.14	
Fig 1	**Average**	0.14	
2A	*Anthoceros agrestis*	0.11	
2B	*Marchantia polymorpha*	0.12	
2C	*Physcomitrium patens*	0.17	
Fig 2	**Average**	0.13	
3A	*Chara*	0.14	
3B	*C. reinhardtii*	0.12	
3C	*D. discoideum*	0.2	Heat
Fig 3	**Average**	0.15	
Fig 4	*D. discoideum*	0.09	H_2O_2
Fig 4	*C. reinhardtii*	0.12	
Fig 4	*Physcomitrium patens*	0.11	
Fig 4	**Average**	0.107	
7A	MDA-MB-231	0.288	Heat
7A	H9c2	0.203	
Fig 7	**Average**	0.245	